The metabolic consequences of glucose-6-phosphate transporter (G6PT) depletion in mice

and

Investigating the role of Transcriptional intermediary factor 1-γ (TIF1γ) in mitosis

By Rachel Fletcher

A thesis submitted to the University of Birmingham

for the degree of Master's of Research (MRes)

UNIVERSITY OF BIRMINGHAM

School of Clinical and Experimental Medicine

College of Medical and Dental Sciences

University of Birmingham

May 2012

Project 1

The metabolic consequences of glucose-6-phosphate transporter (G6PT) depletion in mice

Abstract

The glucose-6-phospate transporter (G6PT) translocates cytosolic glucose-6-phosphate (G6P) into the endoplamic/sacrcoplamic reticulum (ER/SR). In the liver, glucose-6-phosphatase metabolises G6P as the terminal step in gluconeogenesis, essential for maintaining fasting blood glucose levels. Conversely, in both muscle and liver G6P can be converted by hexose-6-phoshate dehydrogenase (H6PDH) to 6-phosphogluconate (6-PG). This process generates the cofactor NADPH which allows 11β-hydroxysteroid dehydrogenase type 1 (11β-HSD1) to reduce cortisone to its active counterpart cortisol. This demonstrates the importance of the G6PT in glucose metabolism and glucocorticoid (GC) activation. H6PDHKO mice have shown GC independent myopathy thought to be attributed to disrupted glucose homeostasis and calcium (Ca^{2+}) metabolism. In this study we used G6PT+/- mice to characterise the effects of G6PT depletion in respect to systematic glucose metabolism when challenged with diabetes inducing high fat diet, and separately the effect on muscle metabolic homeostasis. We found that G6PT depletion may promote weight gain and systemic insulin resistance despite normal fasted glucose levels on high fat diet. Furthermore, we found elevated intracellular Ca^{2+} in G6PT+/- primary muscle cells. As we show 11β-HSD1 enzyme activity was unaffected in G6PT+/- mice we propose novel GC-independent roles for G6PT in controlling glucose and calcium homeostasis.

Ackknowledgements

I would like to thank Dr Gareth Lavery and Dr Craig Doig for their continuous support and advice which has been enabled me to learn so much during this project. I would additionally like to thank everyone on the 2nd floor of the IBR, particularly Emma McCabe, Agnieszka Zielinska, Phil Guest and Dr Stuart Morgan for all their help within the laboratory.

Contents

1. Introduction

1.1. Metabolic disease

Metabolic syndrome is a collection of metabolic disorders that together increase an individual's risk of developing type 2 diabetes mellitus and cardiovascular disease. These metabolic abnormalities include insulin resistance, hyperglycaemia, central obesity and hypertension [1]. The considerable increase in prevalence of metabolic syndrome in recent years has made it a major worldwide public health concern [2]. Insulin resistance is thought to be the primary mechanism by which metabolic syndrome develops, however there is still much to be learned concerning the pathogenesis and progression of metabolic syndrome [3]. Further understanding of the metabolic pathways involved in energy homeostasis is necessary to reduce the detrimental impact of these diseases.

1.2. Glucocorticoids (GC) and metabolism

Cortisol, the predominant GC in humans, is secreted from the adrenal cortex both permissively and adaptively in response to chronic stress and plays an essential role in carbohydrate, fat and protein metabolism [4][5]. Within muscle and fat tissues cortisol opposes the actions of insulin and stimulates glycogenolysis; it also acts anabolically in the liver to stimulate gluconeogenesis [5][6]. Together these actions help to maintain glucose homeostasis and provide the brain with sufficient levels of glucose [6]. The importance of regulating cortisol levels can be demonstrated clinically in patients with cortisol excess such as those with Cushing's syndrome or deficiency such as in Addison's disease. Cushing's patients characteristically present with an overproduction of cortisol with symptoms including central obesity, diabetes and hypertension [7] where as Addison's

disease presents with cortisol deficiency form adrenal failure with typical symptoms of anorexia and hypotension [8].

As Cushing's syndrome patients typically present with similar diagnostic features to those with metabolic syndrome it was proposed that deregulated cortisol levels may play a key role in the pathogenesis of metabolic syndrome. Preliminary studies have shown that in metabolic syndrome cortisol levels are typically raised, but following the reduction of cortisol levels through weight loss, clinical symptoms of metabolic syndrome can be ameliorated [9]. Although further studies are necessary to distinguish the effects of weight loss from reduced cortisol levels before any conclusions can be drawn, this research supports previous studies suggesting that inhibition of cortisol activity may prove to be a valuable therapeutic approach for metabolic syndrome.

GC levels are modulated both systematically and at tissue level. The hypothalamic-pituitary-adrenal (HPA) axis provides systematic regulation and allows elevated cortisol levels in response to chronic stress. Cortisol levels are normally tightly regulated by negative feedback to the hypothalamus and anterior pituitary [10]. GC levels are also controlled at tissue level by the enzyme 11β-hydroxysteroid dehydrogenase type 1 (11β-HSD1). 11β-HSD1 is expressed in metabolic tissues such as liver, adipose and skeletal muscle. It primarily shows reductase activity and thereby converts inactive cortisone (11-dehydrocorticosterone (11-DHC) in mice) into active cortisol (corticosterone in mice) as opposed to its dehydrogenase activity where the conversion is reversed [11].

1.3. G6PT - H6PHD - 11β-HSD1 pathway

The regulation of 11β-HSD1 is complicated by its subcellular location within the endoplasmic/sarcoplasmic reticulum (ER/SR). The ubiquitously expressed glucose 6-

phosphate transporter (G6PT), also known as solute carrier family 37 member 4 (SLC37A4), is the first component of the metabolic triad, which locally regulates GC activation, and consists of G6PT, hexose-6-phosphate dehydrogenase (H6PDH) and 11β-HSD1 (figure 1.1) [12]. Together these components allow the transport of glucose-6-phosphate (G6P) in to the lumen of the ER and subsequent enzyme-mediated GC regeneration. Firstly G6P is transported from the cytosol into the ER via the G6PT; an ER associated antiporter [13][14]. G6P acts as a substrate for H6PDH and is subsequently converted into 6-phosphogluconate (6-PG), concurrently H6PDH reduces $NADP^+$ to NADPH. This allows a high enough NADPH to $NADP^+$ ratio within the ER to sufficiently promote 11β-HSD1 reductase activity and therefore results in GC activation [12].

Moreover, the G6PT - H6PDH - 11β-HSD1 pathway has been considered of great importance towards both characterising and targeting therapies at the group of increasingly prevalent metabolic conditions, particularly obesity and insulin resistance. As excess GC levels can cause unwanted disruption to metabolic homeostasis, inhibition of the enzymes involved in glucocorticoid activation may prove to be a valuable therapeutic strategy to target metabolic diseases [15][16]. Previous animal studies have indicated that 11β-HSD1 inhibitors may show physiological efficacy. Currently 11β-HSD1 inhibitors are in phase II clinical trials to assess their ability to ameliorate these metabolic diseases [15]. However, it is possible that any beneficial effect on metabolism, by the inhibition of 11β-HSD1 mediated GC activation, may be counteracted by the HPA axis which may stimulate increased cortisol release by the adrenals to maintain circulatory cortisol levels.

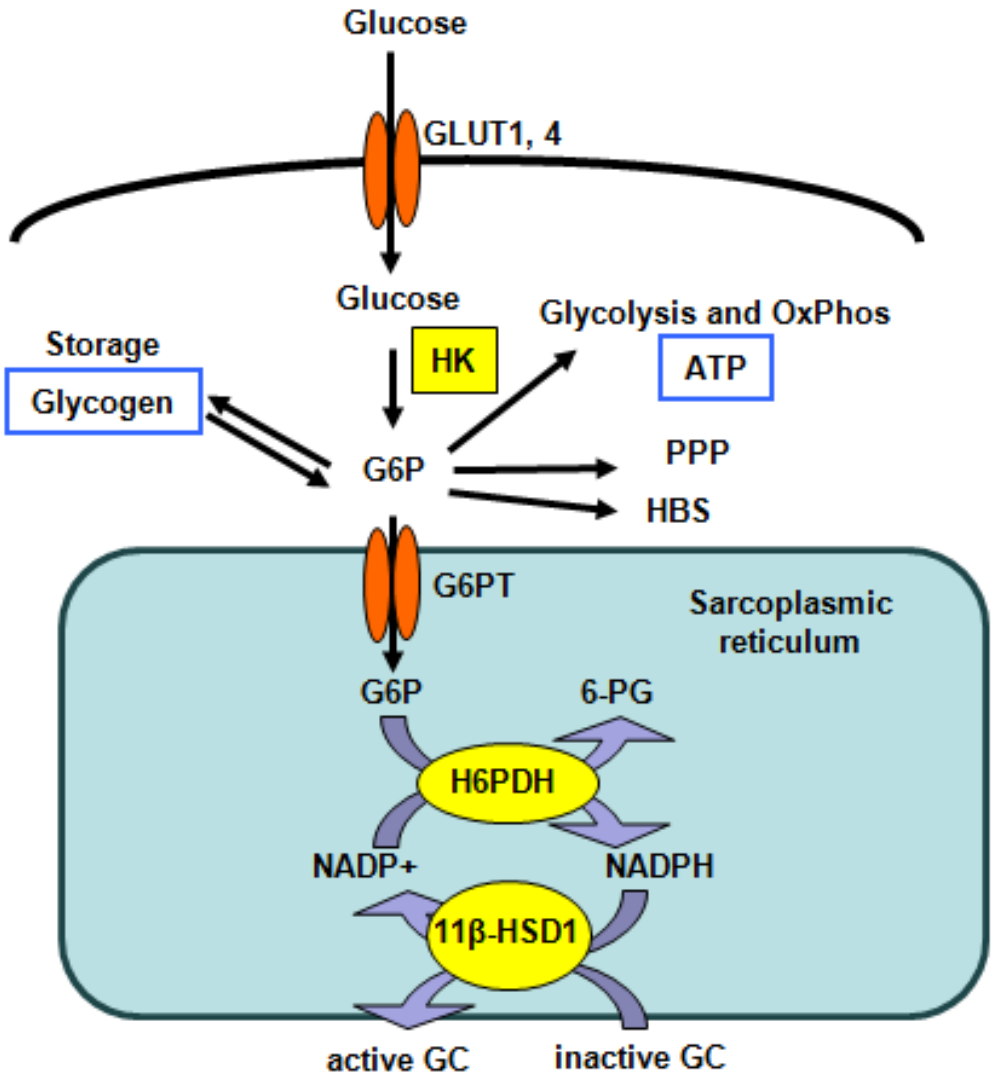

Figure 1.1. The G6PT-H6PHD-11β-HSD1 pathway

A summary of the G6PT-H6PDH-11-βHSD1 system integrated within cellular metabolism. G6P is translocated by the G6PT and metabolised by H6PDH and downstream 11β-HSD1 reductase activity is stimulated allowing GC activation [12].

1.4. Hepatic glucose metabolism

Gluconeogenesis allows glucose to be produced from non-carbohydrate molecules such as pyruvate, glycerol and lactate, and ensures sufficient blood glucose levels are maintained during fasting [6]. Specifically in gluconeogenic tissues, such as the liver, D-glucose-6-phospatase (G6Pase) is expressed in the ER lumen and works in parallel with the G6PT - H6PHD - 11β-HSD1 pathway [17]. In hepatic tissue, G6P is transported into the ER lumen by the G6PT, however here G6P also acts as a substrate for the G6Pase enzyme which catalyses the hydrolysis of G6P into glucose and inorganic phosphate. As this hydrolysis reaction is the final step in both gluconeogenesis and glycogenolysis, the G6Pase system plays an essential role in glucose homeostasis [17]. Figure 1.2 illustrates interactions between the pathways discussed in regards to glucose and GC homeostasis.

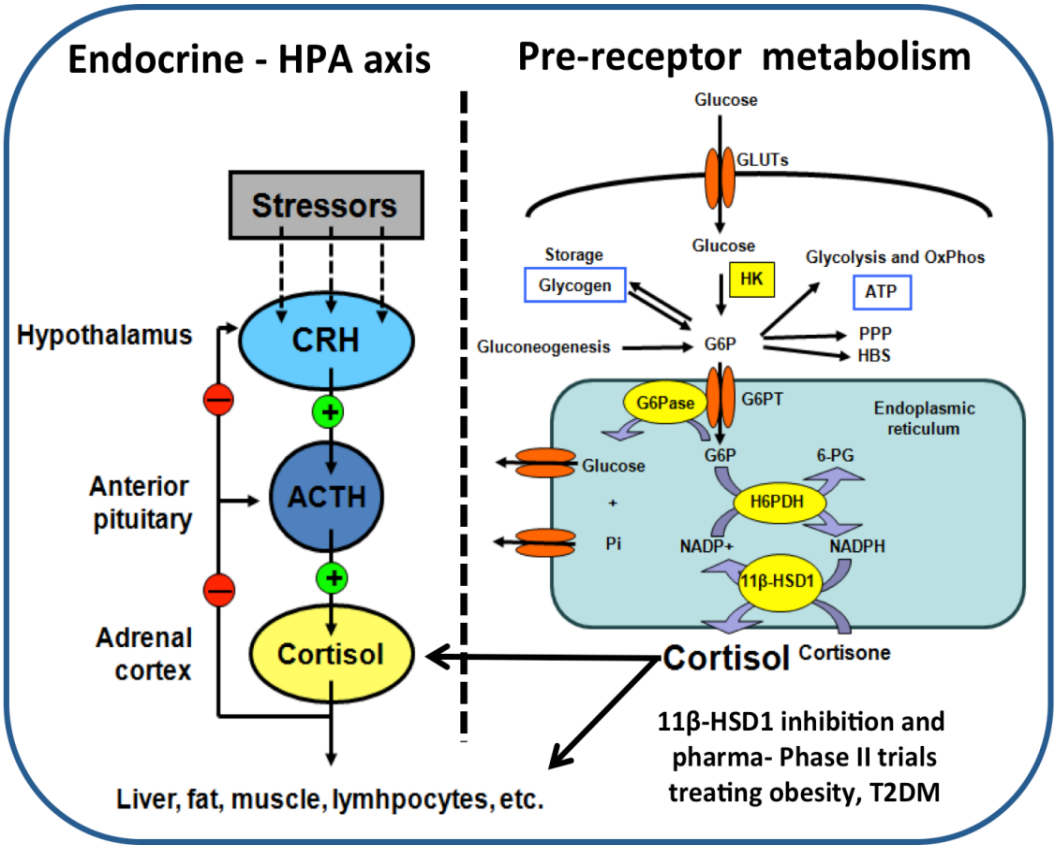

Figure 1.2. Systemic and local GC regulation
An illustration to demonstrate GC regulation through the integration of the endocrine system and pre-receptor metabolism. The role of the hepatic G6Pase system is also shown [12][17].

1.5. Glycogen storage disease type 1a and 1b

Glycogen storage disease type 1 (GSD-1) or von Gierke disease, groups a series of autosomal recessive metabolic disorders associated with abnormalities to the G6Pase system. Deficiencies to G6Pase and the G6PT cause GSD-1a and GSD-1b respectively [13]. Currently more than 85 mutations to the human G6Pase gene have been identified, and over 80 mutations to the G6PT gene have been found. For both genes the mutations identified are mostly missense, small gene alterations with few mutations occurring with considerable frequency [18]. As both these ER associated proteins work collectively to modulate glycaemia, abnormalities to either tend to present with similar malfunctions associated with deregulated energy metabolism. For both disorders patients typically manifest with hypoglycaemia, hepatomegaly, growth retardation and renal dysfunction all of which are characteristic of deficient G6Pase activity. However GSD-1b patients also manifest with neutropenia and neutrophil dysfunction [13]. As expression of G6Pase is specific to gluconeogenic tissues such as the liver, intestine and kidney yet G6PT is ubiquitously expressed it is thought to have alternative unknown roles at these tissues particularly those which exert little glucocorticoid activity. Previous studies using G6PT KO mice gave adverse symptoms similar to GSD-1 patients where complete depletion of the G6PT proved difficult for long term survival of the mice [19].

1.6. H6PDH and HSD1 knockout (KO) mice

Numerous transgenic mouse models have been developed to investigate the effects of 11β-HSD1 inhibition. Both 11β-HSD1KO and H6PDHKO mice, which display a considerable reduction in glucocorticoid sensitivity, show ameliorated glucose homeostasis and resist obesity when fed a high fat diet [12][20]. In contrast, a model overexpressing 11β-HSD1 specifically in adipose tissue presented a metabolic syndrome phenotype including

hypertension, obesity and insulin resistance. Furthermore overexpression of 11β-HSD1 in the liver presents with mild hepatic insulin resistance but with no visceral obesity [21] [22]. These *in vivo* models further support the idea of inhibiting 11β-HSD1 enzyme activity as a novel therapy to improve or reverse the detrimental effects induced by metabolic syndrome in humans.

However, despite the positive metabolic effects seen within these mouse models, H6PDH null mice have demonstrated a severe progressive skeletal myopathy. The myopathy displays increased insulin dependent uptake of glucose, glycogen accumulation and switching of sketetal type II fibres to type I slow twitching fibres in skeletal muscle. These changes are physiologically supported by the diminished running wheel activity and isolated skeletal muscle force generation of the null mice. In addition, the muscles are seen to contain numerous intrafibrillar membraneous vacuoles and aberrant triads which join T tubules to a SR. Expression levels of SR proteins, that participate in the regulation of calcium metabolism, such as calrecticulin and sarcoplasmic/endoplasmic reticulum calcium ATPase (SERCA) also appear to be abnormal. Concurrently, overexpression of genes which encode proteins associated with the unfolded protein response (UPR) pathway was observed [23]. These studies suggest that the G6PT - H6PHD - 11β-HSD1 pathway plays an essential role in muscle homeostasis. However, studies using a 11β-HSD1/H6PDH double KO (DKO) found that GC metabolism and HPA axis regulation was similar to 11β-HSD1 mice yet the DKO mice presented with similar myopathy to the H6PDHKO suggesting the effects are GC independent [24].

H6PDH is expressed exclusively in the ER/SR and functions to catalyse the reduction of G6P in the initial stages of the pentose phosphate pathway. As $NADP^+$ is reduced to

NADPH in concert with G6P reduction is both pathways, H6PDH activity is likely to be integral to the maintenance of an appropriate redox environment within the ER. Disruption to the $NADP^+$ /NADPH ratio by reduced H6PDH activity may alter the ER oxidation-reduction balance, which is necessary for the correct folding of proteins, and result in ER stress [23].

1.7. ER stress

The ER offers proteins optimal conditions for efficient folding and assembly. ER stress can be caused by numerous factors including; a build up of misfolded proteins, altered oxidation-reduction state, depleted glucose levels and disturbed Ca^{2+} homeostasis. In response to ER stress the cell undergoes an unfolded protein response (UPR); whereby the transcription of genes that regulate protein folding is stimulated. Consequently translation of further proteins is halted and chaperone levels are upregulated to assist with correct folding of proteins. Activating transcription factor (ATF6), protein kinase RNA-like endoplasmic reticulum kinase (PERK) and Inositol-requiring1 (IRE1) dissociate from immunoglobulin heavy chain-bindng protein (BiP) and become activated. ATF6 translocates to the nucleus and promotes the expression of UPR genes. In contrast, IRE1 and PERK undergo oligomerisation and autophosphorylation. Phosphorylated IRE1 catalyses the splicing of XBP1 mRNA forming a potent transcription factor for UPR genes, whilst phosphorylated PERK interacts with eukaryotic translation initiation factor 2,α subunit (eIF2α) which reduces the rate of translation. Moreover, Endoplasmic-reticulum-associated protein degradation (ERAD) is upregulated to degrade misfolded proteins beyond repair [25].

Due to the overexpression of UPR proteins and Ca^{2+} disturbances seen in the H6PDHKO mice it has been proposed that the disruption to muscle homeostasis and consequent myopathy may be, at least partly, a result of SR stress [23].

1.8. What is the role of G6PT in metabolic homeostasis and muscle function?

To date studies of the glucocorticoid activation pathway have predominantly focused on characterising the effects of knocking down the two enzymes, however to get a clearer picture of the pathway, by removing the G6P upstream substrate, through knocking out the G6PT will ensure that no alternative compensatory pathways can reduce G6P and provide NADPH for 11β-HSD1 activation in the ER. In addition by preventing G6P flux into the ER it will help to determine alternative roles for G6P within this organelle.

Previous studies have used G6PT antisense oligonucleotides (ASO) in diabetes db/db mice and found G6PT reduction ameliorated hyperglycaemia and insulin resistance; as 11β-HSD1 expression was consequently reduced it is proposed these effects are GC dependent [26].

To further assess the role of G6PT in metabolism a heterozygous transgenic mouse model for the G6PT has been established. Characterisation of this heterozygous model will determine whether the beneficial effects of reducing GC activity can be seen without muscular pathology. To do this we will first look at the role of the G6PT in regards to whole body glucose homeostasis which we postulate to be GC dependent. We will examine clinical differences between heterozygous and wild type mice on a high fat diet to establish whether the heterozygous model can ameliorate obesogenic effects and insulin resistance. In addition, to determine the role of the G6PT specifically in muscle homeostasis, which we propose to be GC independent, we will examine the metabolic

status of primary isolated muscle cells from heterozygous and wild type mice. Elucidating the importance the G6PT in this pathway will help to determine potential new therapeutic targets of metabolic syndrome whilst recognising possible adverse effects from disrupting this pathway such as altered muscle homeostasis.

1.9. Hypothesis and Aims

We hypothesise that reduced G6PT expression will lead to reduced HSD1 mediated Glucocorticoid generation and ameliorate high fat diet induced insulin resistance. We hypothesise that G6PT expression is an important regulator of G6P metabolism and skeletal muscle homeostasis

A heterozygous G6PT mouse model has been developed to further investigate its importance in metabolic homeostasis. The aims of this project are:

1) To characterise the metabolic phenotype of G6PT +/- mice on a high fat diet to establish systemic effects of G6PT depletion using *in vivo* analysis of glucose clearance and body weight as well as molecular analysis of liver and muscle tissue.
2) To investigate the role of the G6PT in muscle homeostasis using G6PT+/- primary myotubes to conduct multiple experiments to assess levels of key metabolites such as ATP, G6P, Ca^{2+} and glycogen as well as determine 11β-HSD1 enzyme activity.

2. Methods

2.1. Transgenic heterozygous G6PT mouse

The G6PT KO allele and embryonic stem cells were made by the European conditional mouse mutagenesis (EUCOMM) programme. Homologous recombination of an insertational mutagenesis cassette at an early intron (seen in figure 2.1) inhibits gene transcription and effectively makes the allele null.

Embryonic stem cells containing the below allele of the G6PT gene were injected in to a blastocyst and implanted into a C57BL/6 mouse. A portion of the parental mouse stem cells within the blastocyst now contain the knockout sequence and upon birth chimeras derived from this knockout containing cassette appear a patchy grey colour. Genotyping was then performed to confirm either heterozygosity or wild type status.

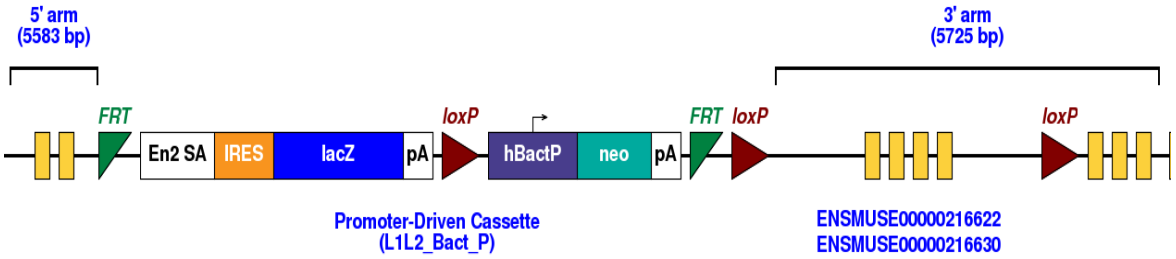

Figure 2.1. The G6PT KO allele – a linear representation of the G6PT KO allele produced by homologous recombination of an insertational mutagenesis cassette.

2.2. Primary Myofibre isolation

Mice were genotyped and culled at 8 weeks old. The Extensor digitorum longus (EDL) muscle was dissected, fully intact, from tendon to tendon as described in Rosenblatt 1995 [27] and placed in Dulbecco's modified Eagle's medium (DMEM) with 0.2% v/v of collagenase and incubated at 37°C for 2 hours. EDL tissue was placed in serum coated cell

culture plates in DMEM preheated to 37°C to equilibrate. Serum coated glass pipettes were used to gently expel cell medium onto the muscle to release individual myofibres. 48 well cell culture plates were coated in Matrigel (BD Biosciences) and incubated at 37°C until the Matrigel had set. Then the individual myofibres isolated from the muscle were transferred onto the set Matrigel plates to grow. (All primary cells incubated at 37°C were in an atmosphere of 5% CO_2)

2.3. Primary cell maintenance

Primary culture maintenance was conducted using the following media. Fibres were seeded in plating media (DMEM with 30% foetal bovine serum (FBS), 10% Horse serum (HS), 1% Chick embryo extract (CEE), 100mg/ml fibroblast growth factor (FGF)) and left for 96 hours at 37°C. Once satellite cells have migrated from the fibre, plating media was removed as well as the primary fibres and proliferation media (DMEM with 10% HS, 0.5% CEE) was added this was changed to differentiation media (DMEM 2% HS, 0.5% CEE) as the myoblasts approached confluence (80%) and myotubes allowed to fully develop for 4 days incubating at 37°C before experimentation (illustrated in figure 2.3).

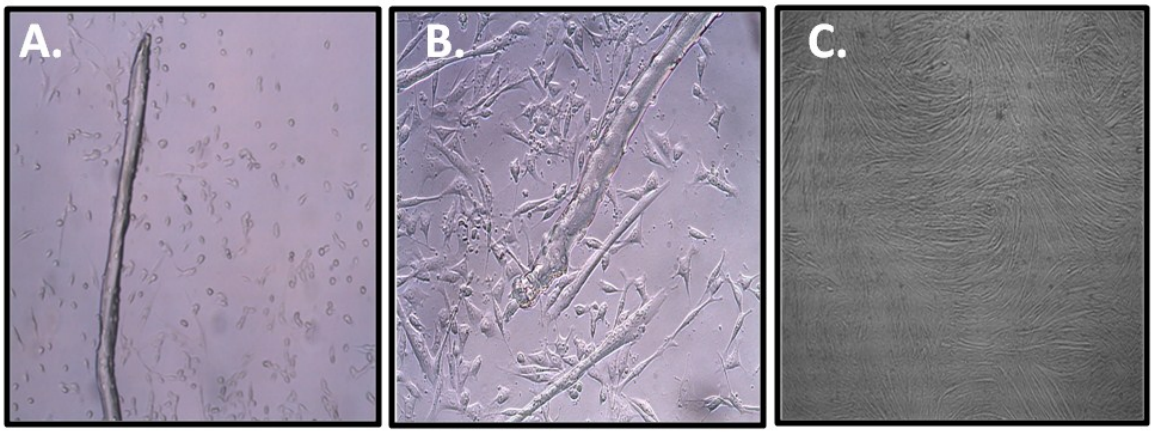

Figure 2.3. Primary muscle cell culture – Light microscopic imaging of satellite cells migrating from the primary myofibre (A), myoblast proliferation and differentiation (B) and mature myotubes (C)

2.4. Genotyping

DNA samples from tail clippings of C57BL/6 mice were prepared for PCR by placing each clipping in 100µl of digestion buffer (50mM Tris (pH 8.0), 100mM EDTA, 100mM NaCl, 1% sodium dodecyl sulphate (SDS)) and 2µl of proteinase K and incubating overnight at 57°C on a hot block. Samples were then vortexed and heated at 98°C for 20 minutes to denature enzymes. Samples were spun down to pellet debris and DNA was amplified using the 2x BioMix Red (Bioline) by following manufacturer's instructions and using the primers listed below. Briefly 1µl of sample DNA was added to 19µl of each master mix, stated in table 2.4, in PCR tubes. Samples were vortexed and placed in the PCR machine set to 3 minutes at 95°C then 35 cycles of {30 seconds 95°C, 30 seconds 60°C and 30 seconds 72°C} followed by 3 minutes at 72°C and left forever at 4°C.

Primers-:

Slc37a4-for – TGCAGCTGGTTACCTGTCAGACAGG

loxR primer – TGAACTGATGGCGAGCTCAGACC

Slc37a4-5'-arm – TCCTTGGTGGATGAGATCGCTCTGG

Slc37a4-3'-arm – TTGTGATGAGCCCTGCAGCGAAGG

LAR3 primer – CAACGGGTTCTTCTGTTAGTCC

LoxP PCR mix/sample	Lar3 PCR mix/sample
Mastermix - 10µl	Mastermix - 10µl
Primer (loxP) - 0.5µl	Primer (3'-arm) - 0.5µl
Primer (slc37a4-for) - 0.5µl	Primer (5'-arm) - 0.5µl
Nuclease free water (NFW)- 8µl	Primer (LAR3') - 0.5µl
	Nuclease free water - 7.5µl

Table 2.4. Genotyping mastermixes

Samples were then loaded on to a 2% (w/v) agarose gel dissolved in TBE (Triboric acid/EDTA) heated and mixed gently to aid dissolution. 1µl/10ml of gel red was added to the mix and the gel was poured into the plates of the electrophoresis apparatus. Well forming combs were placed into the top and the gel was left to set. Combs were then removed and samples were loaded into the wells; 10 µl of BenchMark™ pre-stained protein ladder (Invitogen) was also loaded as a molecular weight marker. The electrophoresis was run at 120 volts for 40 minutes. Gels were then removed from the apparatus and bands were visualised under UV conditions.

2.5. Colourimetric and fluorometric assays

Media was aspirated from 2 wells of primary cells from 48 well plates and each of the metabolic assays (listed in table 2.5) were performed following the manufacturer's instructions (Cambridge Bioscience). Briefly, cells were lysed in the buffer provided in the assay kit and scraped from the well surface and placed into Eppendorf tubes. Equal volumes of lysate were placed in wells of a 96 well plate and the appropriate reagents provided by the kit were added. In parallel to this, standards were made using known concentrations of the metabolites. Absorbance, at the appropriate wavelength, for each sample was read using a colourimeter and metabolite concentrations for each sample were determined by extrapolating the absorbance from their respective standard curve.

Assay name	Company	Catalogue number
Glycogen assay kit	Cambridge Bioscience	K646-100
Calcium colorimetric assay kit	Cambridge Bioscience	K380-250
ATP colorimetric/fluorometric assay kit	Cambridge Bioscience	K353-100
Glucose-6-phosphate assay kit	Cambridge Bioscience	K657-100

Table 2.5. List of colourimetric and fluorometric assays

A Fura-2 fluorometric assay (Invitrogen) was also used to determine Ca^{2+} levels by following manufacturers instructions. Briefly assay reagents were applied directly to the cultured primary myotubes in 96 well plates in order and after the appropriate incubations fluorescence was measured.

2.6. Immunoblotting

To harvest protein 1ml of a 10ml RIPA buffer stock (50mM Tris, 150mM NaCl, 1% NP40, 0.5% sodiumdeoxycholate and 0.1% SDS) (supplemented with 100µl of phosphatase inhibitor and 1 tablet of protease inhibitor) was added to each well. Cells were then scraped from the plate surface and transferred to an Eppendorf tube; lysates were kept on ice at all times unless stated otherwise. The samples were then subject to freeze thaw conditions to improve lysis and centrifuged for 10 minutes. The lipid pellet was discarded and the supernatant was transferred to a new tube.

Sample protein concentration was then determined using the Quick Start™ Bradford assay kit (Bio-Rad). 5µl of each sample and BSA protein standards (of known concentrations in RIPA buffer) were added to wells of a 96well plate. 200µl of BioRad protein assay reagent B was added to each well followed by 25µl of BioRad protein assay reagent A (supplemented with 20µl of reagent 5 per 1ml of reagent A to correct for the presence of SDS in RIPA buffer).

Sodium dodecyl sulphate-polyacrylaminde gel electrophoresis (SDS-PAGE) was used to separate the protein samples by molecular weight. 12% w/v acrylamide gels (from 40% acrylamide stock, 0.1M Tris, 0.1M bicine (N,N-bis(2-hydroxyethyl)glycine), 0.1% w/v SDS, 0.25 % TEMED (N,N,N',N'-tetramethylethylenediamine) and, added last, 0.06% ammonium persulphate (APS)) were mixed and poured into electrophoresis apparatus,

with combs placed into the top to form wells, and left to polymerise. Then, on removal of the combs, wells were washed and filled with running buffer (0.1M Tris pH 7.4, 0.1M bicine, 0.01% w/v SDS). Wells were loaded individually with 20µg/ml protein samples or a protein ladder used to estimate the size of bands once the gel is run. Once loaded the apparatus lid was placed on and filled with running buffer and the gels were then electrophoresed at 120volts for 1.5 hours. Gels were transferred to a nitrocellulose membrane using the iBlot (Invitrogen). Primary antibody (G6PT 1:5000 (Santa Cruz), β-actin 1:10000 (Sigma), SERCA2 1:1000 (Cell signaling), α-tubulin 1:2000 (Santa Cruz)) in 5% milk was added to the membrane and left on a shaker overnight at 4˚C, the membrane was washed in Tris-buffered saline with Tween 20 (TBS-T) (0.1% v/v Tween^{TM} 20, 0.2M sodium chloride and 0.02M Tris (pH 7.6)) and secondary antibody in 5% milk was added (anti-mouse 1:10000 (for G6PT) and anti-rabbit-HRP 1:10000 (for SERCA2) (Dako)) and incubated on a shaker for 2 hours at RT. The membranes were then washed for 15 minutes 4 times in TBS-T and subsequently exposed to ECL luminance substrate according to manufactures instructions (Bio-Rad) and wrapped in saran film and exposed to blue-xray film (Wolt laboratories) in a developing cassette and placed in the xograph developer.

2.7. In vivo - high fat diet

10 Mice (4 wild type, 6 G6PT+/-) were fed high fat pellets (60% fat) for 9 weeks and weighed twice weekly. On week 6 the mice were subjected to a glucose tolerance tests (GTT) with weight differences adjusted by the injected glucose concentration (2U/kg). Tail bleeds were carried out to read blood glucose concentration using a glucometer every 30 minutes.

At week 10 mice were culled by cervical dislocation and quadricep, soleus, TA and liver tissue was collected by dissection and frozen immediately in liquid nitrogen for future analysis.

2.8. 11β-HSD1 activity assay

To test for 11β-HSD1 activity the conversion of inactive 11-DHC to active corticosterone is measured. Tissue explants and primary myotubes were used. For the primary myotubes media was removed and 1ml of Serum free DMEM was added to the wells. For the tissue explants around 20mg pieces were weighed and added to individual wells containing 1ml of serum free DMEM media. The samples were incubated at 37°C in a 5% CO_2 atmosphere for 30 minutes. Then 20,000 cpm/reaction of radioactive ^{3}H-11-DHC and 100nM of 11-DHC was added to each well. Muscle tissue and primary cells were incubated for 6 hours and liver tissue was incubated for 2 hours, all at 37°C in 5% CO_2. Following the respective incubation periods the media from each well was transferred into a glass tube and 5ml of dichloromethane was added and the solution was briefly vortexed. Subsequently samples were centrifuged at 15,000rpm for 15 minutes to enable the extraction of the steroids. After this the upper aqueous phase was aspirated from the samples which were then placed under an air blowing sample concentrator (Techne) set at 55°C to allow evaporation of the remaining organic phase which contains the steroids. Samples were resuspended in 50µl of dichloromethane and briefly vortexed. Then using a Pasteur pipette each sample was spotted on silica coated thin layer chromatography plate (Thermofisher), 2cm above the base and with 1.5cm gaps between samples. 5µl of non-radiolabelled 10mM 11-DHC/corticosterone in ethanol was additionally spotted to provide a running control. The plate was run in a tank with 200ml (90:10) of chloroform:absolute ethanol for 1 hour 15 minutes to separate the steroids. On separation the radioactivity of

^{3}H-11-DHC and its converted product ^{3}H-corticosterone was determined using a Bioscan Imaging scanner (LabLogic). The correct peaks were identified by referring to the position of the cold steroids under UV light. The percentage of inactive 11-DHC converted to active corticosterone was calculated to establish enzyme activity given as the pmole of steroid converted per gram of tissue per hour (pmol/g/h).

2.9. RNA extraction

Tissue samples were homogenised in 1ml of thiocyanate-phenol (Trizol) using a mechanical homogeniser; with the blade cleaned in ethanol between samples. Alternatively, for primary cells, 1ml of Trizol was added to the wells and mixed by pipetting up and down. Cells were scraped from the surface and placed into Eppendorf's and left for 5 minutes at room temperature (RT). 200µl of chloroform was added and after vortexing samples were left for 5 minutes at RT. Samples were centrifuged for 5 minutes at 12,000rpm at 4°C and the top layer of each sample was transferred into a new Eppendorf. 500µl of isopropanol (propan-2-ol) was then added to the new tubes which were inverted 5 times and left, for RNA precipitation, at -20°C for 30 minutes. Nucleic acid was pelleted by centrifugation at 12000rpm at 4°C and the isopropanol was removed. Samples were washed in 75% ethanol and left to dry before they were resuspended in nuclease free water (NFW). The RNA was quantified using the NanoDrop (ND, labtech international) and assessed for RNA integrity (with a 260/280 nm ratio between 1.7 and 2 deemed good). The samples were stored at -80°C until further use.

2.10. Reverse transcription

RNA was reverse transcribed to cDNA using the High capacity cDNA reverse transcription kit (Applied Biosystems, USA) following the manufacturers protocol. Briefly, a master mix was prepared with the volumes of reagents stated in table 2.10 per sample.

2x Reverse transcription master mix / sample
10 x RT buffer - 2µl
25 x dNTP mix (100mM) – 0.8µl
10 x RT random primers - 2µl
MulitiScribe™ reverse transcriptase - 1µl
RNase inhibitor - 1µl
Nuclease free water – 3.2µl

Table 2.10. Reverse transcription mastermix

10µl of the 2x master mix was added to 100µl tubes with 10µl of RNA (1µg/10µl). Samples were then mixed gently and centrifuged briefly before they were placed in the thermal cycler. Settings for the thermal cycler were; 10 minutes at 25°C, 120 minutes at 37°C, 5 minutes at 85°C and then continuously at 4°C.

2.11. Real time PCR (qPCR)

Primers for genes of interest were thawed on ice and covered from light. Master mixes, consisting of 5µl 2x qPCR master mix (Applied Biosystems), 3.5µl NFW and 0.5µl gene primer probe (listed in table 2.11), were made for each of the genes tested. All cDNA samples were run in triplicate with 1µl of cDNA added to each well of a 384 well plate followed by 9µl of the appropriate gene master mix. Plates were sealed with film and

briefly centrifuged before loading on the ABI 7500 Real Time-PCR machine at pre-set settings.

Gene	Primer probe Cat.# (applied biosystems)
G6PT	Mm00484574_m1
H6PDH	Mm00557617_m1
HSPa5	Mm00517690_g1
ITGB1BP3	Mm01172899_g1
Calr	Mm00482936_m1
PEPCK	Mm01247058_m1
HSD11b1	Mm00476182_m1
G6Pase	Mm00839363_m1

Table 2.11. List of the genes used for qPCR analysis

2.12. Statistics

Prism6 (GraphPad) was used for statistical analysis of data given as mean±SEM, with statistical significance given to P values <0.05. Groups were compared using t-test analysis for metabolic, RT-PCR and activity assays (n numbers are stated in their respective figure legend). Mean ΔCt values were used for qPCR statistical analysis. Two way ANOVA was used for GTT analysis. (Key: * = P<0.05, ** = P<0.01, *** = P<0.001).

3. Results

3.1. G6PT genotype

Tail clipping samples were taken from mice and we used PCR to amplify the sample DNA and subsequently ran samples on an agarose gel. The genotype of each mouse was then determined by assessing the bands on the gel. The 5' and 3' primers allow synthesis of WT cDNA which consists of 678 base pairs where as the Lar3' primer allows synthesis of cDNA from the inserted cassette which consists of 482 base pairs. Figure 3.1 shows sample F1 with two bands, representing the presence of the WT gene (band between 600 and 700 base pair region) and the inserted cassette (band between the 400 and 500 base pair region), indicative of a heterozygous genotype. F2 has just one band between the 600 and 700 base pair region which indicates a WT genotype. Positive (+) and negative (-) controls were also used during genotyping to confirm primer efficiency and integrity.

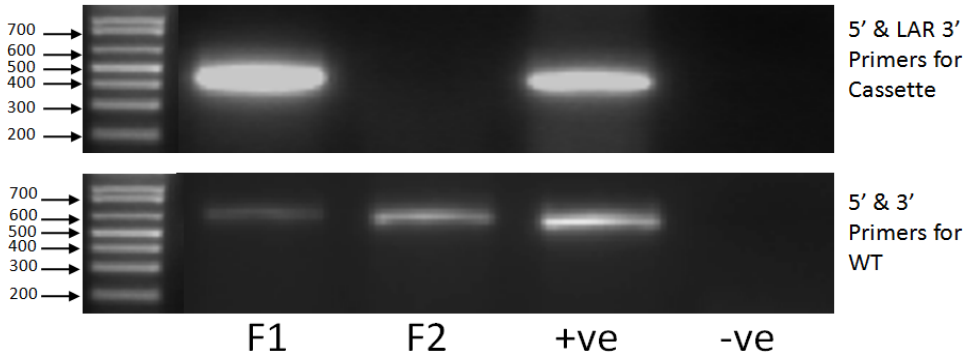

Figure 3.1. Genotyping for heterozygous G6PT mice
Mice tail clips were genotyped by running amplified DNA samples on an agarose gel. Heterozygous genotype is indicated by two bands (WT and inserted cassette) (F1) and Wild type genotype was indicated by a single band WT band (F2) and is determined WT. Positive (+ve) and negative (-ve) controls were also used.

3.2. G6PT mRNA expression levels

To assess whether the heterozygous G6PT mice showed differences in transporter levels compared to wild type we analysed the G6PT gene expression. RNA was extracted from liver and quadricep tissue samples of the high fat diet (HFD) mice and reverse transcribed to cDNA for qPCR analysis. Figure 3.2 shows that G6PT gene expression trends downwards in liver and is significantly reduced in quadriceps of HFD fed G6PT+/- mice.

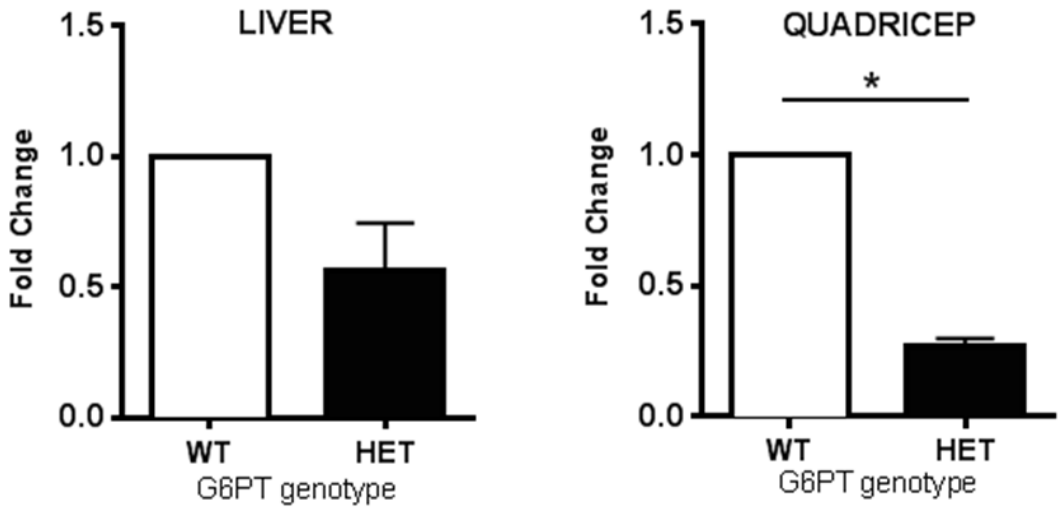

Figure 3.2. G6PT mRNA expression in tissue
G6PT expression levels were analysed by qPCR in liver and quadricep tissue from G6PT+/- and WT mice on a high fat diet. G6PT expression was significantly reduced in quadriceps of G6PT+/- mice (n=3, p= <0.05).

3.3. Physiological phenotype of HFD fed G6PT+/-

To investigate the induction of insulin resistance in G6PT+/- and WT when fed a high fat diet we looked for physiological differences *in vivo*. The mice were fed a high fat diet for 6 weeks and weighed twice weekly. Over this time period the G6PT+/- mice had a significantly larger percentage increase in body weight compared to the WT (Fig 3.3.A). In

addition, at the end of this 6 week period we performed a fasting glucose tolerance test (GTT) and found that the G6PT+/- mice had a reduced ability to clear glucose compared to WT. Figure 3.3.B demonstrates that after 15 minutes there is a similar increase in blood glucose concentration after the glucose injection in both mice. In the WT mice a normal glucose response was then seen with the glucose concentration beginning to reduce at 30 minutes post injection and at the 120 minute time point levels of blood glucose return to those similar to pre-injection levels. However at the 30 minute time point in the G6PT+/- mice the blood glucose concentration is still rising by 60 minutes it begins to reduce but at a much slower rate compared to the WT group. From 30mins until the 120 minute time point the G6PT+/- blood glucose concentration is significantly higher than the WT and, unlike the WT, the blood glucose does not return to pre-injection levels after 120 minutes.

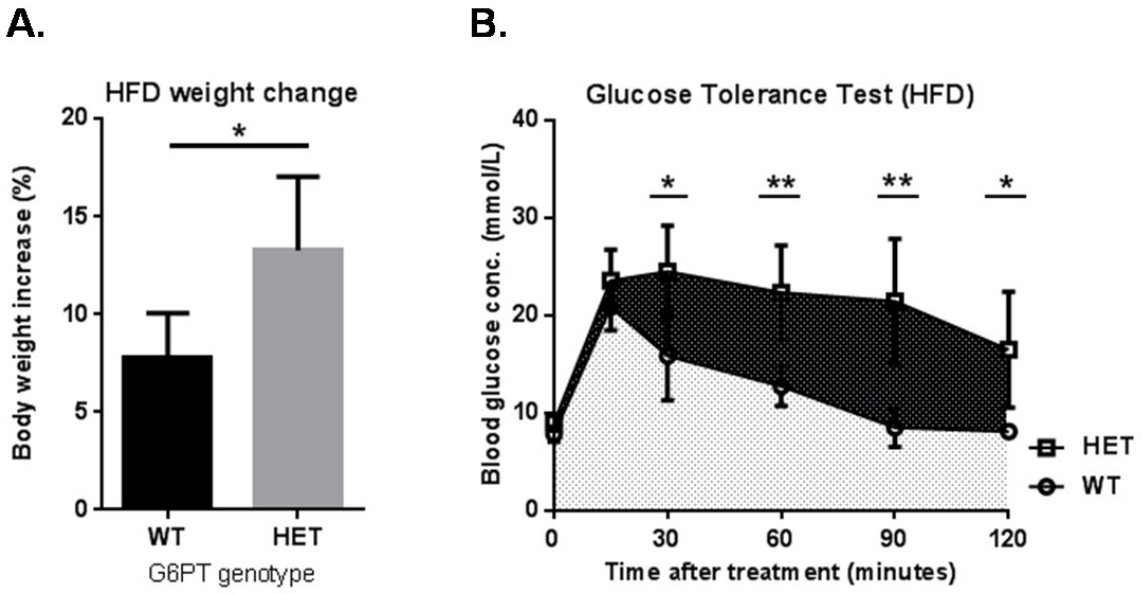

Figure 3.3 Physiological phenotype of HFD fed G6PT+/- mice

(A) shows the percentage of weight gain in G6PT+/- HFD fed mice was significantly higher than WT and (B) shows G6PT+/- and WT mice response to GTT; the ability of HFD fed G6PT +/- mice to clear glucose appears impaired compared to WT (WT n=4 and G6PT+/- n=6).

3.4. Metabolic phenotype of HFD fed G6PT+/-

To initially investigate whether the expression levels of any metabolic genes of interest may be altered in HFD fed G6PT+/- mice, liver and quadricep tissue was collected from the mice. RNA was extracted from the tissue and reverse transcribed to cDNA for quantitative PCR analysis.

Firstly we looked at the expression levels of H6PDH and 11β-HSD1 in order to establish whether reduced expression of G6PT may alter the expression levels of the enzymes downstream of the G6PT in the pathway. The gene expression levels of H6PDH and 11β-HSD1 were not significantly different in the G6PT+/- liver or quadricep, although 11β-HSD1 expression did appear slightly increased compared to the WT (figure 3.4.1).

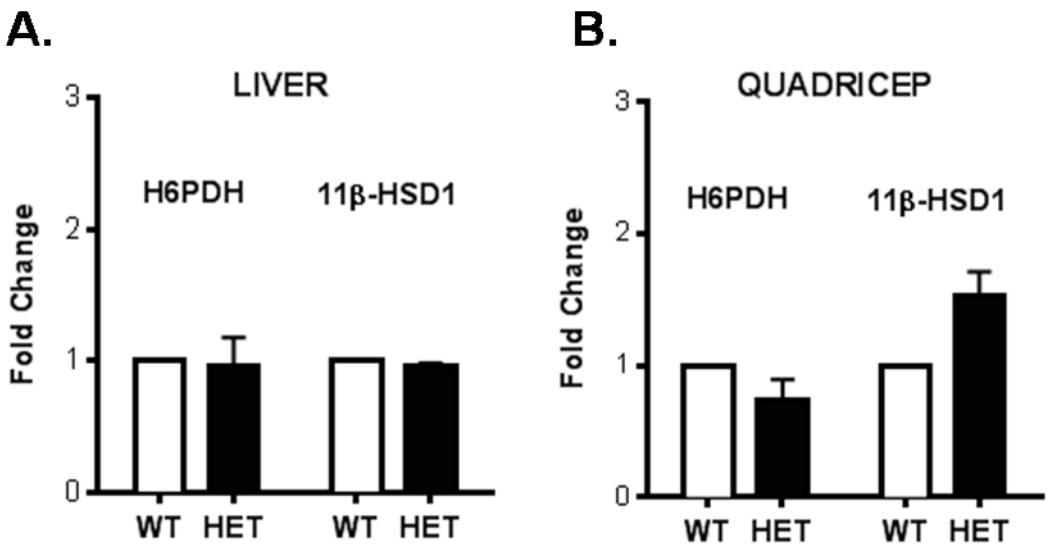

Figure 3.4.1 H6PDH and 11β-HSD1 mRNA expression in G6PT+/- mice

H6PDH and 11β-HSD expression levels were analysed by qPCR in liver (A) and quadricep (B) tissue from G6PT+/- and WT mice on a high fat diet. There was no significant change to enzyme expression in G6PT+/- compared with WT mice (n=3).

Following previous studies where the myopathy seen in the H6PDHKO mice was proposed to be the consequence of ER stress [23] we looked at the gene expression of ER related proteins. Heat Shock protein a5 (HSPa5), also known as BiP, and calreticulin (Calr) are involved in protein folding mechanisms and therefore used as markers of ER stress[28][29]. Both these genes showed no significant change in expression in both quadricep and liver tissue although levels did appear to be slightly reduced (Figure 3.4.2.A).

ITGB1BP3 is a gene involved in the negative regulation of muscle differentiation, whereby overexpression prevents terminal differentiation and maintains the proliferative ability of cells [30]. Therefore we investigated expression levels to indicate changes to muscle growth and homeostasis between the WT and heterozygous mice in the quadricep tissue. Expression levels of ITGB1BP3 showed no significant change between WT and heterozygous genotypes (Figure 3.4.2.C).

Additionally we examined the expression levels of gluconeogenic genes in hepatic tissue to determine whether reduced G6PT may affect hepatic glucose homeostasis. G6Pase and PEPCK, both of which encode enzymes involved in the gluconeogenesis pathway [31], showed no significant difference in gene expression levels between WT and G6PT+/- in liver tissue (Figure 3.4.2.B).

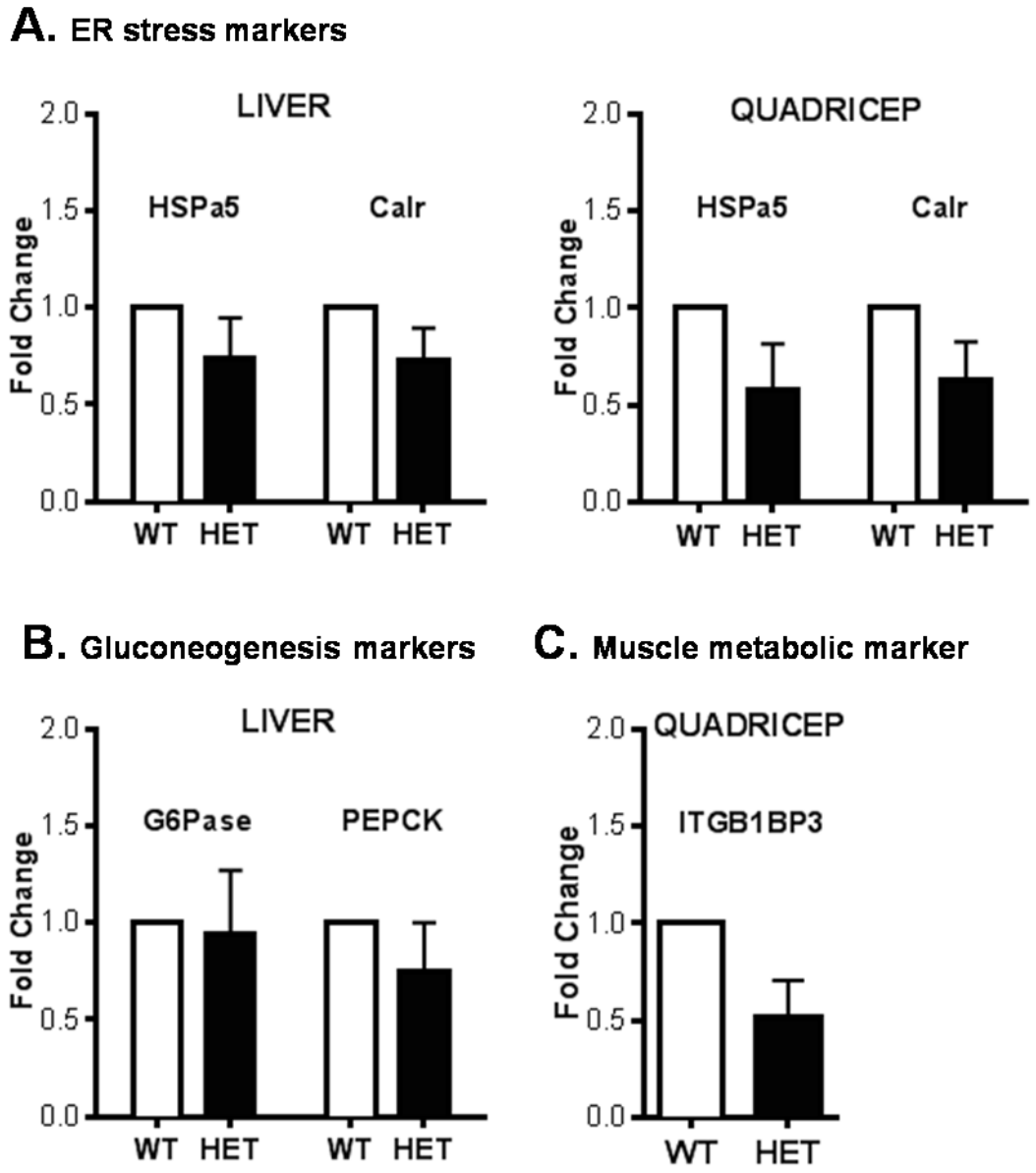

Figure 3.4.2 mRNA expression of metabolic markers in HFD fed G6PT+/- mice

Expression levels of key metabolic markers were analysed by qPCR. (A) shows expression levels of ER stress markers to be unchanged in liver and quadriceps tissue, (B) shows that gluconeogenic markers in liver tissue are unchanged and (C) shows the muscle metabolic marker ITGB1BP3 gene expression to be also unchanged in HFD fed G6PT+/- mice (n=3).

3.5. 11β-HSD1 enzyme activity in HFD fed G6PT+/-

We used 11β-HSD1 activity assays to determine whether a reduction in G6PT expression caused changes to 11β-HSD1 activity in the G6PT+/- mice compared to the WT. Using radio labelled 11-DHC this assay establishes the rate at which 11-DHC is converted into corticosterone, thereby assessing the enzyme activity. Figure 3.5 shows that in both liver and quadricep tissue there was no significant difference in the conversion rate of inactive 11-DHC into active corticosterone between WT and G6PT+/- mice on a HFD.

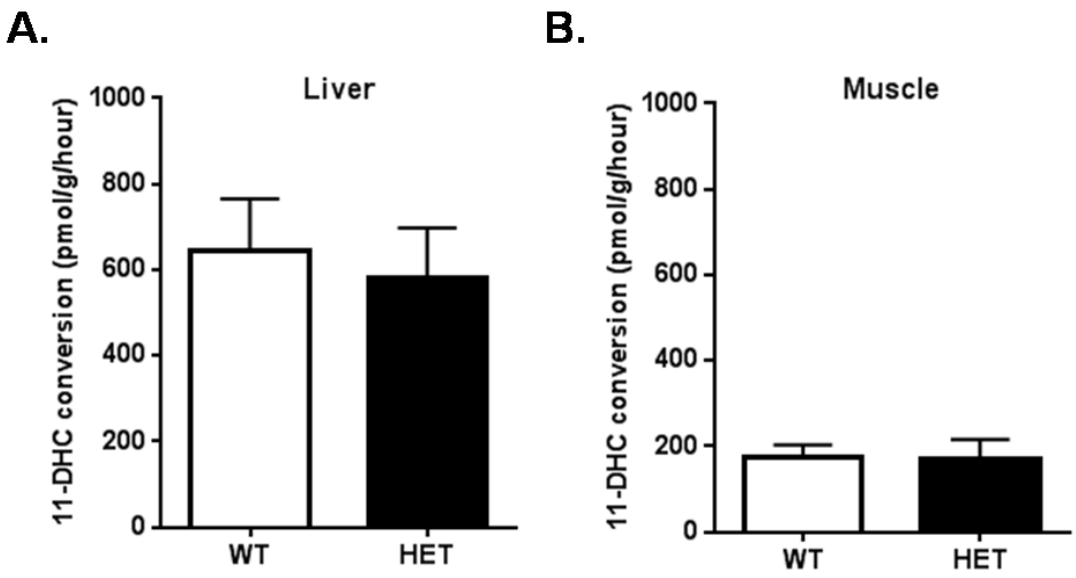

Figure 3.5. 11β-HSD1 enzyme activity in G6PT+/- mice

11β-HSD activity is represented by its conversion of 11-DHC to corticosterone. There was no significant change to enzyme activity in liver (A) or quadricep (B) tissue explants from G6PT+/- mice on a high fat diet compared with WT mice (WT n=4, G6PT+/- n=6).

Having completed the *in vivo* analysis we then wanted to explore in more detail the known pathophysiology seen in the H6PDHKO mice where it has been proposed that the myopathy detected in these mice may be attributed to ER stress and disrupted Ca^{2+} signalling. Therefore we investigated whether similar changes were seen in muscle cells isolated from G6PT+/- mice [24].

3.6. Primary muscle cell G6PT protein expression

To assess whether the changes to the G6PT gene expression levels seen in tissue samples from the HFD mice are followed by reduced protein levels of the G6PT we investigated the protein levels of the transporter in primary myotubes. Protein was extracted from the primary myotubes and separated by SDS-PAGE. Western blotting for the G6PT, and β-actin as a loading control, allowed qualitative indications of protein expression levels. Figure 3.6. shows that protein levels for the G6PT appear to be reduced in the primary myotubes isolated from G6PT+/- mice compared to levels in the WT. These findings correlate with the reduction in G6PT gene expression levels observed previously in liver and quadricep tissue harvested from HFD fed G6PT+/- mice (Figure 3.2).

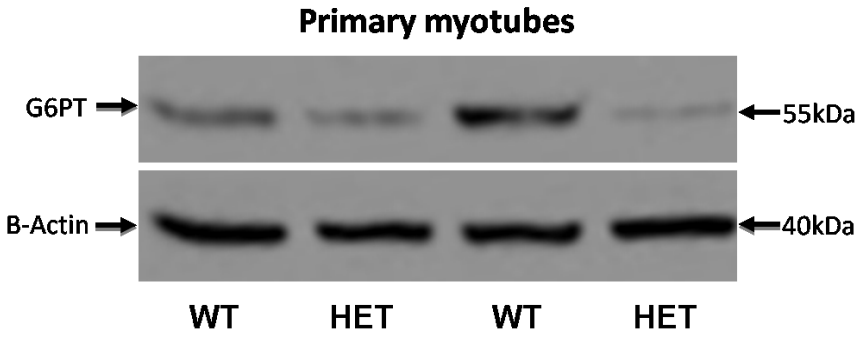

Figure 3.6. G6PT protein expression in primary myotubes
Protein from primary myotubes was analysed by immunoblotting. G6PT levels appear considerably reduced in G6PT+/- myotubes compared to WT. B-Actin was used as a loading control (n=2).

3.7. 11β-HSD1 enzyme activity in G6PT+/- primary myotubes

We also used the 11β-HSD1 activity assay to determine whether a reduction in G6PT expression caused changes to 11β-HSD1 activity in primary myotubes isolated from the G6PT+/- mice. Figure 3.7 shows that the conversion rate of inactive 11-DHC into active corticosterone in the heterozygous G6PT myotubes does not appear to differ from the WT myotubes. This suggests that 11β-HSD1 enzyme activity is not altered in G6PT+/- myotubes.

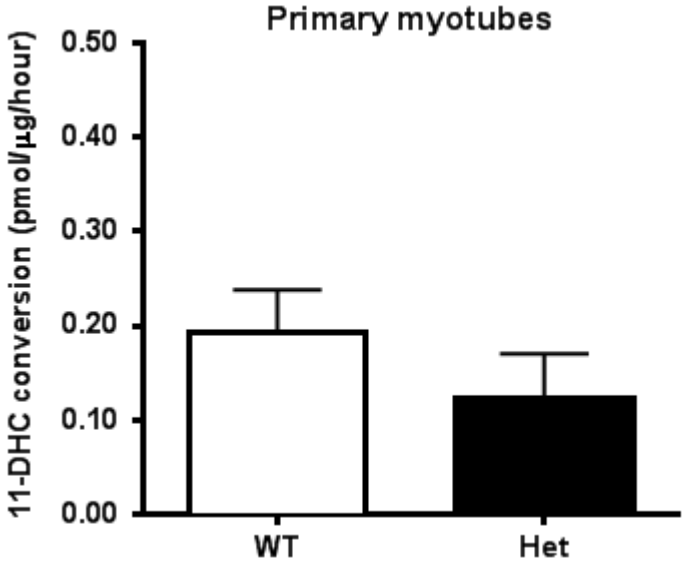

Figure 3.7. 11β-HSD1 enzyme activity in G6PT+/- myotubes
11β-HSD activity is represented by its conversion of 11-DHC to corticosterone. There was no significant change to enzyme activity in the G6PT+/- primary myotubes compared with WT (n=6).

3.8. Metabolic effects of reduced G6PT in primary muscle cells

To investigate whether reduced G6PT expression in G6PT+/- mice may cause changes to muscle homeostasis we measured the intracellular levels of key muscle metabolites glycogen, ATP and Ca^{2+} in the satellite cell derived myotubes using colourimetric and

fluorometric assays. Both glycogen and ATP levels are unchanged in WT and G6PT+/- primary muscle cells (Figure 3.8.A and B). However Ca^{2+} concentrations in the G6PT+/- myotubes are significantly increased compared to WT levels (Figure 3.8.C). Using a colourimetric assay we also tried to measure G6P levels however the results were negative in both WT and heterozygous samples; this was attributed to the requirement of immediate perchloric acid treatment to deproteinize harvested cells. This is to be revisited as part of future studies.

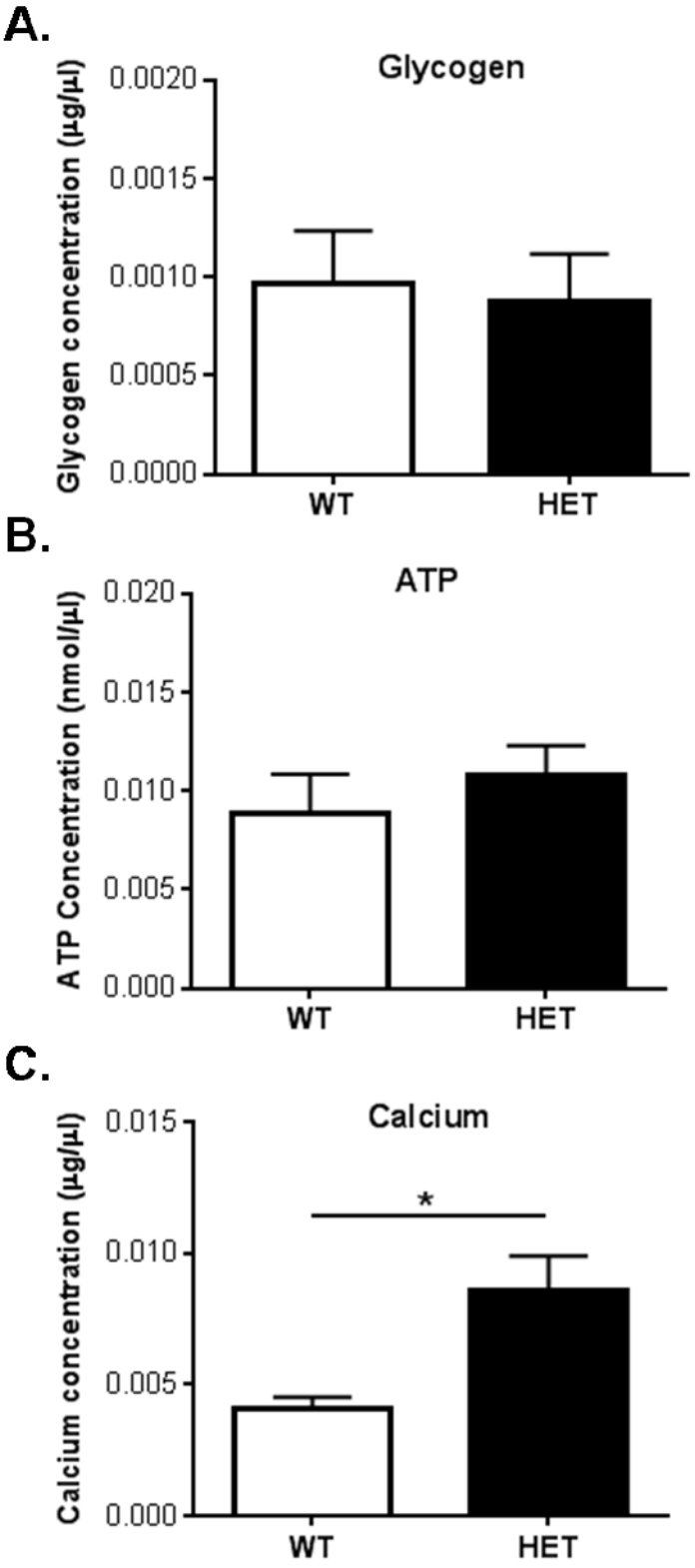

Figure 3.8. Levels of key muscle metabolites in myotubes of G6PT+/- mice

Colourimetric and fluorimetric analysis of key metabolites showed that glycogen (A) and ATP (B) levels remained unchanged, yet Ca^{2+} (C) levels were significantly increased in G6PT+/- myotubes (n=5 (A) ,n=3 (B) and n=6 (C)).

3.9. Regulation of calcium in primary muscle cells

From the Ca^{2+} colourimetric assay Ca^{2+} levels appeared increased therefore we used the fura-2 assay as an alternative method to verify these changes. This allowed quantification of free intracellular Ca^{2+}; where a shift in the excitation wavelength of fura-2 can be seen upon binding of Ca^{2+}. The assay reagents were added directly to primary myotubes in 96 well plates and fluorescence excitation was read. From the results in figure 3.9.A free Ca^{2+} levels appear to be raised in the G6PT+/- primary myotubes compared with the WT myotubes and therefore corroborate with our previous colourimetric assay results.

Sarco/endoplasmic reticulum Ca^{2+}-ATPase (SERCA) 2 is a Ca^{2+} ATPase and allows the reuptake of Ca^{2+} from the cytosol into the SR [32]. Thus, to further investigate the Ca^{2+} status of the primary myotubes, we examined SERCA2 protein expression levels by western blotting. The results in figure 3.9.B. indicate that, concurrent with intracellular free Ca^{2+} levels, SERCA2 protein levels are upregulated in $G6PT^{+/-}$ myotubes.

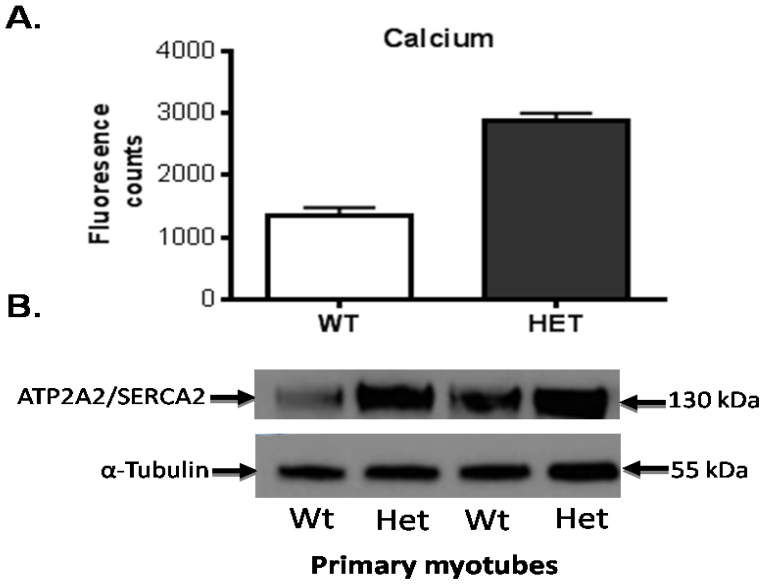

Figure 3.9. Levels of intracellular calcium and SERCA2 protein expression in myotubes of G6PT+/- mice
(A) Using the FURA-2 assay we showed an upward trend in free intracellular calcium levels in G6PT+/- myotubes (n=2). (B) By immunoblot analysis an increase in SERCA2 protein expression in G6PT+/- myotubes (n=2).

4. Discussion

The G6PT translocates G6P from the cytosol into the ER/ SR lumen. In the liver, G6P can be metabolised by G6Pase in the terminal step of gluconeogeneis liberating glucose to maintain glycemia. However, in both liver and muscle G6P can be converted to 6-phosphoglucolactone by H6PDH, generating NADPH as a cofactor. The NADPH generated permits the enzyme 11β-HSD1 to reduce cortisone to the active GC cortisol, and maintain a cycle of NADP/ NADPH for the local luminal environment. Thus the G6PT stands as a regulator of the ER/ SR luminal environment in terms of G6P and glucose metabolism, GC production and redox cycling. In support of this, H6PDHKO mice, whilst being GC insensitive, also develop a GC independent myopathy associated with altered glucose homeostasis and disturb Ca^{2+} metabolism [23].

This study has focussed on characterising mice heterozygous for a null G6PT allele and examined the hypothesies firstly, that decreased G6PT can reduce hepatic glucose production and ward off glucose intolerance associated with obesity through GC dependent and independent mechanisms. Secondly, that G6PT depletion in primary muscle cells promotes metabolic disturbances that partly explain the myopathy seen in H6PDHKO mice.

4.1. Heterozygous G6PT expression

We demonstrated a significant reduction of G6PT mRNA and protein expression in heterozygous mice, and can infer that knocking out one allele of the G6PT does lead to a reduction in expression. We would expect that this would consequently decrease the amount of G6P transport from the cytosol to the ER/SR, which is thought to be G6PT dependent in muscle [13][18].

4.2. *In vivo* and *ex vivo* analysis for global metabolic characterisation of the G6PT+/- genotype

To induce obesity and diabetes (hyperglycemia), G6PT+/- mice were fed a high fat diet. A principle mechanism of diabetes in high fat feeding is increased hepatic glucose output as a consequence of insulin resistance. G6PT+/- mice accumulated a greater proportion of body weight during the study, and were considerably less glucose tolerant as compared to control mice. These results do not support our hypothesis that reduced G6PT and consequently reduced G6P flux may cause a reduction in the activity of the enzymes within the pathway that would result in decreased GC activation and reduce glucose release through the activity of the G6Pase. As elevated GC levels are associated with weight gain [33] we would have expected the G6PT+/- mice to gain less weight on the high fat diet and additionally show increased ability to clear glucose. These thoughts are also supported by previous findings, where reduction in hepatic G6PT by anti sense oligo (ASO) treatment resulted in amelioration of hyperglycaemia and insulin resistance [26]. Also from H6PDHKO studies where 11β-HSD1 dehydrogenase activity results in GC inactivation, KO mice presented with reduced weight gain and improved glucose tolerance [34]. As this is not the case here it may indicate that alternative GC independent pathways may be affected by the reduction of G6P flux within the ER. All the mice used in this study were the same age at starting but the G6PT+/- mice were slightly heavier at the beginning of the study, and therefore it may be argued that the weight differences, prior to the high fat diet, could be due to differences attributed by changes to G6PT levels and predisposing them to increased weight gain despite the high fat diet. If the G6PT+/- mice are less able to regulate their energy metabolism then they may be more prone to weight gain even on a normal diet. In addition the fasting glucose levels for the heterozygous mice were similar

to those of the WT mice suggesting weight differences may not entirely account for differences in glucose clearing ability. Further weight monitoring of future litters is required to establish whether a trend between weights and genotype actually exists.

Our results suggest that there is no obvious difference in 11β-HSD1 enzyme activity in tissue explants from the WT and G6PT+/- mice, indicating that the reduction in levels of G6PT does not cause significant downstream changes to enzyme activity within the liver or skeletal muscle, and it is likely that G6P flux would need to be substantially reduced to incur significant changes to the rate of GC activation. Previous studies using ASO to significantly reduce G6PT mRNA and protein levels have shown that on adequate reduction of the transporter there is a decrease in downstream activity of H6PDH and 11β-HSD1 [19][26]. Thus, the results from the 11β-HDS1 activity assay support our prediction that any physiological changes seen in the G6PT+/- mice are independent of GC levels and may be due to alternative pathways that G6P plays a role within.

H6PDH and 11β-HSD1 gene expression in both liver and skeletal muscle tissue also appeared unchanged. These results reinforce the enzyme activity data and show that it is unlikely that the enzyme activity is maintained by increased expression of either enzyme to compensate for the possible reduced G6P flux into the ER/SR. The results also indicate that the extent of G6PT expression reduction in G6PT+/- mice is not adequate to stimulate reduced expression of the downstream enzymes.

As the G6PT is a key component of the G6Pase system and acts in concert with G6Pase in gluconeogenic tissues, alterations to G6PT levels may have an effect on gluconeogenic processes in the ER. Studies by Wang et al. in diabetic (db/db) mice have demonstrated that disruption to the hepatic G6PT-H6PDH-11β-HSD1 system using the GC antagonist

RU486 exhibits changes to hepatic glucose metabolism with a significant down regulation of PEPCK seen compared to control groups [35]. Therefore we looked at gene expression levels of gluconeogenic markers G6Pase and PEPCK in the study to detect possible changes to glucose metabolism in hepatic tissue of G6PT+/- mice. The gene expression levels of G6Pase and PEPCK appeared unchanged in the liver of heterozygous G6PT mice. These results imply that despite changes to G6PT mRNA levels, which may result in reduced G6P influx, there is no indication of disruption to gluconeogenesis in the G6PT+/- mice.

Previously, studies proposed that ER/SR stress may be triggered by alterations to the G6PT-H6PDH-11β-HSD1 system due to changes to the redox environment of the ER/SR. In skeletal muscle of H6PDHKO mice an overexpression of genes involved in the UPR pathway suggested SR stress, which has been proposed to contribute to subsequent myopathy [23]. Data from the gene expression analyses also appear to show no significant change to UPR markers Calreticulin and HSPa5. This indicates that ER stress has not been induced by reduced G6PT expression in the G6PT+/- skeletal muscle and liver tissue. In addition, another gene greatly dysregulated in H6PDHKO muscle, ITGB1BP3 [12], was not significantly different in G6PT+/- quadriceps muscle tissue compared with the WT indicating again the normal functioning of muscle growth and differentiation pathways.

4.3. *In vitro* analysis of the role of the G6PT in muscle homeostasis

Utilising primary myotubes derived from G6PT +/- mice we were able to specifically investigate the role of the G6PT in regulating non GC dependent aspects of muscle homeostasis. As our results show a down regulation in G6PT+/- protein levels we investigated the possible effects of this in the primary myotubes.

In corroboration with the results we found in quadriceps muscle tissue, 11β-HSD1 enzyme activity in the primary myotubes does not appear to be changed. This supports our proposal that the reduced protein expression of the G6PT seen in the G6PT+/- primary myotubes is not sufficient enough to alter downstream enzyme activity.

In H6PDHKO muscle, glycogen storage is increased and ATP decreased [12]. Assays in primary G6PT+/- myotubes showed no obvious changes in levels compared to control myotubes. Despite the physiological differences seen *in vivo*, the G6PT+/- mice appeared able to function relatively normally and there were no obvious symptoms to indicate severe pathology of the heterozygous mice, for that reason we would not anticipate any major differences in the intracellular glycogen and ATP levels of primary myotubes.

We were unable to successfully determine the G6P levels in primary myotubes isolated from WT and G6PT+/- mice. This may have been due to continued enzyme activity post harvesting, which may have consumed or converted G6P. As a result further investigation, by using revised methods whereby samples are deproteinised immediately after lysis, is required.

The final parameter to test was Ca^{2+} homeostasis, as in H6PDHKO mice, in which G6PT is down-regulated 5 fold [12], Ca^{2+} signalling is defective, and increased intracellular Ca^{2+} is observed. Our data show a trend towards increased intracellular Ca^{2+} levels. The data from the colourimetic assay showed a significant increase in intracellular Ca^{2+} levels. This was followed up with a fura-2 assay which specifically measures free intracellular Ca^{2+} levels and the results appear to correspond with those from the colourimetric assay. Although the fura-2 assay tested substantial populations of myotubes with little variability between the fluorescence counts in WT and heterozygous groups, only 2 biological primary myotube

replicates were available. Therefore repetition of this experiment is necessary to confirm whether these changes are significant.

Ca^{2+} is a key intracellular metabolite involved in a vast range of signalling cascades and therefore to ensure appropriate functioning of cells Ca^{2+} levels are highly regulated [36]. Tight regulation of Ca^{2+} is particularly important in muscle due to its role in contraction; SERCA pumps assist to maintain appropriate intracellular free Ca^{2+} levels by storing it in the SR [32]. Our results show that, in corroboration with increased free intracellular Ca^{2+}, SERCA2 protein levels appeared to be increased in the G6PT+/- mice. Therefore the suggested changes to Ca^{2+} levels in G6PT+/- mice may be due to dysregulation of Ca^{2+} uptake into the SR. It may be expected that upregulation of SERCA2 would result in lower free Ca^{2+} changes but it is possible that the increased presence of SERCA2 may be stimulated by excessive free Ca^{2+} levels in order to maintain levels. It would be interesting to see changes to both free Ca^{2+} and SERCA2 expression over time to elucidate whether upregulation of SERCA2 does ameliorate the changes to intracellular Ca^{2+} levels.

In addition, a role for the G6PT in regulating Ca^{2+} has previously been identified in other tissues whereby gene silencing of G6PT decreased sphingosine-1-phosphate mediated Ca^{2+} mobilisation in glioblastoma cells [37]. A role for the G6PT had also been found in ATP dependent ER/SR Ca^{2+} sequestration where G6P has been shown to enhance Ca^{2+} sequestration [38]. Therefore, increased Ca^{2+} levels in our study may be explained by reduced G6P levels which may impair SR uptake of Ca^{2+} from the cytosol. Furthermore, studies have shown that genetic deficiencies in G6PT, which results in GSD-1b, present with impaired neutrophil chemotaxis which it has been proposed from G6PT-/- mice studies may be a consequence of abnormal Ca^{2+} flux in neutrophils [39]. Together these

studies illustrate a role for G6PT, beyond G6P transport, in regulating intracellular Ca^{2+} homeostasis. This may account for the changes to Ca^{2+} levels in the G6PT+/- primary myotubes. Further research regarding Ca^{2+} signalling is necessary to subsequently establish whether these changes are likely to contribute to myopathy seen in H6PDHKO mice or be a consequence of it.

In conclusion, the results suggest that the G6PT+/- genotype does not appear to ameliorate high fat diet induced insulin resistance. Contrary to our hypothesis, reduced G6PT may actually promote whole body insulin resistance. Despite the apparent reduced expression of G6PT, downstream 11β-HSD1 enzyme activity appears unchanged in both skeletal muscle and liver. Therefore suggesting a reduced G6PT flux has no effect of downstream enzyme activity and thus no change in GC activation. However, reduced G6PT may cause altered muscle intracellular Ca^{2+} levels; a key metabolite in the maintenance of muscle homeostasis which therefore supports our hypothesis that the transporter plays a key role in GC independent skeletal muscle homeostasis.

4.4. Limitations

It is notable that results in this project are limited due to the short time period allocated for this project. This project was intended to provide preliminary data towards characterising the heterozygous G6PT mouse line in which any key findings could be further investigated. As a result of time limitations the *in vivo* high fat diet study was carried out on mice that were readily available from the start of the project despite differences in the average starting weight of the two groups. Ideally, had time permitted, the mice would have been placed on the high fat diet for greater than 12 weeks, and additional *in vivo* investigations would have been carried out including insulin sensitivity tests and muscle

strength. In addition, increased replicates would have been preferable if the appropriate mice had been available.

Furthermore, had time allowed, we would have assessed G6PT protein levels in tissue to see if they correlated with the mRNA expression data and the G6PT protein levels in the primary myotubes. Additionally, it would have been useful to examine gene expression levels of other skeletal muscle tissues other than the quadriceps. This would have helped determine whether our gene expression results are consistent in quadriceps and EDL muscle and if we had compared quadricep, soleus and tibialis anterior (TA) muscle we could have determined whether G6PT+/- induced fibre type specific effects. Finally, though technically demanding, it will be useful to develop a direct G6PT transporter activity assay in tissue, to ascertain the level of ER/ SR flux achieved when G6PT expression is reduced.

It must also be appreciated that the model systems used in both *in-vivo* and *in vitro* to characterise the role of G6PT have limitations. Although using transgenic mice allowed us to make global metabolic comparisons between genotypes in a higher organism; it is key to firstly recognise that there are vast metabolic differences between humans and rodents. In addition, the use of mice made it difficult to control potential confounding factors in the study of energy metabolism such as the amount of energy intake by food and expenditure by exercise of each mouse. Similarly, whilst the isolated primary myotubes provide a useful model to indicate skeletal muscle activity and homeostasis, it is important to acknowledge that *in vivo* there is vast communication between neighbouring and distant tissues which may counteract or compensate for the changes seen in isolated tissues.

4.5. Future prospects

From this research we would look to further investigate the Ca^{2+} phenotype of the heterozygous G6PT model and aim to gain a better understanding of the relationship between the G6PT and Ca^{2+} within this metabolic pathway. In addition, the development of a muscle specific G6PT KO model would be the next major step for this research. The muscle specific knockout will provide a more direct understanding of the role of G6PT within the pathway and additionally allow better understanding of the importance of the pathway as a whole in relation to both insulin sensitivity and metabolic homeostasis in skeletal muscle. The specificity of the knockout will define pathology caused solely by changes to muscle homeostasis without interference from the hepatic system. In all, this further research will help towards our long term aims to establish both potential benefits and consequences of regulating GC activation at tissue level by targeting the G6PT pathway. We envisage that a better understanding of the pathways involving the G6PT may be applied clinically towards the development of novel therapeutic and preventative strategies against insulin resistance and myopathy.

5. References

1. Deedwania, P. & Gupta, R. Management issues in the metabolic syndrome. *The Journal of the Association of Physicians of India* **54**, 797–810 (2006)
2. Eckel, R., Grundy, S. & Zimmet, P. The metabolic syndrome. *Lancet* **365**, 1415–28 (2005)
3. Saely, C., Rein, P. & Drexel, H. The metabolic syndrome and risk of cardiovascular disease and diabetes: experiences with the new diagnostic criteria from the International Diabetes Federation. *Hormone and metabolic research = Hormon- und Stoffwechselforschung = Hormones et métabolisme* **39**, 642–50 (2007)
4. Tataranni, P. *et al.* Effects of glucocorticoids on energy metabolism and food intake in humans. *The American journal of physiology* **271**, E317–25 (1996)
5. Dinneen, S., Alzaid, A., Miles, J. & Rizza, R. Metabolic effects of the nocturnal rise in cortisol on carbohydrate metabolism in normal humans. *The Journal of clinical investigation* **92**, 2283–90 (1993)
6. Oh, K.-J., Han, H.-S., Kim, M.-J. & Koo, S.-H. Transcriptional regulators of hepatic gluconeogenesis.*Archives of pharmacal research* **36**, 189–200 (2013)
7. Tabarin, A. & Roger, P. [Cushing's syndrome: diagnostic exploration]. *Presse médicale (Paris, France : 1983)* **23**, 43–8 (1994).
8. Krysiak, R. & Okopień, B. [Adrenal insufficiency].*Wiadomości lekarskie (Warsaw, Poland : 1960)* **65**, 108–23 (2012)
9. Anagnostis, P., Athyros, V., Tziomalos, K., Karagiannis, A. & Mikhailidis, D. Clinical review: The pathogenetic role of cortisol in the metabolic syndrome: a hypothesis. *The Journal of clinical endocrinology and metabolism* **94**, 2692–701 (2009)
10. O'Connor, T., O'Halloran, D. & Shanahan, F. The stress response and the hypothalamic-pituitary-adrenal axis: from molecule to melancholia. *QJM : monthly journal of the Association of Physicians* **93**, 323–33 (2000)
11. Tomlinson, J. *et al.* 11beta-hydroxysteroid dehydrogenase type 1: a tissue-specific regulator of glucocorticoid response.*Endocrine reviews* **25**, 831–66 (2004)
12. Zielinska, A., Walker, E., Stewart, P. & Lavery, G. Biochemistry and physiology of hexose-6-phosphate knockout mice. *Molecular and cellular endocrinology* **336**, 213–8 (2011).

13. Chou, J., Matern, D., Mansfield, B. & Chen, Y.-T. Type I glycogen storage diseases: disorders of the glucose-6-phosphatase complex. *Current molecular medicine* **2**, 121–43 (2002)
14. Pao, S., Paulsen, I. & Saier, M. Major facilitator superfamily.*Microbiology and molecular biology reviews : MMBR* **62**, 1–34 (1998).
15. Gathercole, L. *et al.* 11β-Hydroxysteroid Dehydrogenase 1: Translational and Therapeutic Aspects. *Endocrine reviews*(2013).doi:10.1210/er.2012-1050
16. Hu, G.-X. *et al.* Curcumin as a potent and selective inhibitor of 11β-hydroxysteroid dehydrogenase 1: improving lipid profiles in high-fat-diet-treated rats. *PloS one* **8**, e49976 (2013)
17. van Schaftingen, E. & Gerin, I. The glucose-6-phosphatase system. *The Biochemical journal* **362**, 513–32 (2002)
18. Chou, J. The molecular basis of type 1 glycogen storage diseases. *Current molecular medicine* **1**, 25–44 (2001)
19. Sloop, K. *et al.* Specific reduction of hepatic glucose 6-phosphate transporter-1 ameliorates diabetes while avoiding complications of glycogen storage disease. *The Journal of biological chemistry* **282**, 19113–21 (2007)
20. Semjonous, N. *et al.* Hexose-6-phosphate dehydrogenase contributes to skeletal muscle homeostasis independent of 11β-hydroxysteroid dehydrogenase type 1. *Endocrinology* **152**, 93–102 (2011)
21. Paterson, J. *et al.* Liver-selective transgene rescue of hypothalamic-pituitary-adrenal axis dysfunction in 11beta-hydroxysteroid dehydrogenase type 1-deficient mice.*Endocrinology* **148**, 961–6 (2007)
22. Lavery, G. *et al.* Lack of significant metabolic abnormalities in mice with liver-specific disruption of 11β-hydroxysteroid dehydrogenase type 1. *Endocrinology* **153**, 3236–48 (2012)
23. Lavery, G. *et al.* Deletion of hexose-6-phosphate dehydrogenase activates the unfolded protein response pathway and induces skeletal myopathy. *The Journal of biological chemistry* **283**, 8453–61 (2008)
24. Semjonous, N. *et al.* Hexose-6-phosphate dehydrogenase contributes to skeletal muscle homeostasis independent of 11β-hydroxysteroid dehydrogenase type 1. *Endocrinology* **152**, 93–102 (2011)

25. Wu, J. & Kaufman, R. From acute ER stress to physiological roles of the Unfolded Protein Response. *Cell death and differentiation* **13**, 374–84 (2006)
26. Du, H. *et al.* Specific reduction of G6PT may contribute to downregulation of hepatic 11β-HSD1 in diabetic mice.*Journal of molecular endocrinology* **50**, 167–78 (2013
27. Rosenblatt, J., Lunt, A., Parry, D. & Partridge, T. Culturing satellite cells from living single muscle fiber explants. *In vitro cellular & developmental biology. Animal* **31**, 773–9 (1995)
28. Michalak, M., Groenendyk, J., Szabo, E., Gold, L. & Opas, M. Calreticulin, a multi-process calcium-buffering chaperone of the endoplasmic reticulum. *The Biochemical journal* **417**, 651–66 (2009)
29. Ni, M. & Lee, A. ER chaperones in mammalian development and human diseases. *FEBS letters* **581**, 3641–51 (2007)
30. Li, J., Mayne, R. & Wu, C. A novel muscle-specific beta 1 integrin binding protein (MIBP) that modulates myogenic differentiation. *The Journal of cell biology* **147**, 1391–8 (1999)
31. Yabaluri, N. & Bashyam, M. Hormonal regulation of gluconeogenic gene transcription in the liver. *Journal of biosciences* **35**, 473–84 (2010)
32. Periasamy, M. & Kalyanasundaram, A. SERCA pump isoforms: their role in calcium transport and disease. *Muscle & nerve* **35**, 430–42 (2007)
33. Morton, N. & Seckl, J. 11beta-hydroxysteroid dehydrogenase type 1 and obesity. *Frontiers of hormone research* **36**, 146–64 (2008)
34. Lavery, G. *et al.* Hypoglycemia with enhanced hepatic glycogen synthesis in recombinant mice lacking hexose-6-phosphate dehydrogenase. *Endocrinology* **148**, 6100–6 (2007)
35. Wang, Y. *et al.* Tissue-specific dysregulation of hexose-6-phosphate dehydrogenase and glucose-6-phosphate transporter production in db/db mice as a model of type 2 diabetes. *Diabetologia* **54**, 440–50 (2011)
36. Berridge, M., Bootman, M. & Roderick, H. Calcium signalling: dynamics, homeostasis and remodelling. *Nature reviews. Molecular cell biology* **4**, 517–29 (2003)
37. Fortier, S., Labelle, D., Sina, A., Moreau, R. & Annabi, B. Silencing of the MT1-MMP/ G6PT axis suppresses calcium mobilization by sphingosine-1-phosphate in glioblastoma cells. *FEBS letters* **582**, 799–804 (2008)

38. Chen, P., Csutora, P., Veyna-Burke, N. & Marchase, R. Glucose-6-phosphate and Ca2+ sequestration are mutually enhanced in microsomes from liver, brain, and heart. *Diabetes***47**, 874–81 (1998)

Project 2

Investigating the role of Transcriptional intermediary factor 1-γ (TIF1γ) in mitosis

Abstract

Transcription intermediary factor 1γ (TIF1γ) is known for its transcriptional regulatory activity. It has previously been shown as a tumour suppressor where disturbances to TIF1γ functioning have been associated with numerous cancers. In this study we show that TIF1γ is post translationally modified by phosphorylation in mitotic cells. From further immunoblot analysis we propose that the PHD-Bromo domain of TIF1γ holds this phosphorylation site, however other TIF1γ domains act as essential binding domains for TIF1γ interacting proteins. By mass spectromic analysis we were able to identify three TIF1γ phosphorylation sites, with phosphorylation at serine 856 specific to mitotic cells. In addition we identified numerous TIF1γ interacting proteins including Cdt1 and Geminin which are known to be important in the regulation of DNA replication. Although furthers studies are necessary to determine the importance of TIF1γ phosphorylation in mitosis, these findings suggest TIF1γ may play a key role in regulating cell cycle progression and DNA replication.

Acknowledgements

I would like to thank Dr Andy Turnell for all of the time, help and advice he has given me throughout this project. I would also like thank Dr Roger Grand, Dr Ashley Martin and Paul Minshall for their support within the laboratory.

Contents

1. Introduction:

1.1. Cancer

Cancer is a disease characterised by uncontrolled cell growth. This normally occurs when control mechanisms for correct and timely mitotic division and cell death are deregulated [1]. Genetic lesions cause damage to the cell cycle checkpoint pathways and promote the gain of function of oncogenes and the loss of function of tumour suppressors[2][3]. Genomic instability and aneuploidy, cells presenting with abnormal numbers of chromosomes, are the main hallmarks of cancer and as a result cellular proliferation may dominate over cellular apoptosis. [1]

Proto-oncogenes play a role in the regulation of cell proliferation, differentiation and apoptosis; when mutations arise in these molecules they can become activated oncogenes leading to uncontrolled proliferation and tumourigenesis [4][5]. Ras is an example of a proto-oncogene seen to be mutated in 25% of all human tumours [1]. It is characterised by its intrinsic guanosine triphosphatase (GTPase) activity which can regulate intracellular signalling pathways. When mutated the GTPase activity of ras becomes constitutively activated leading to cellular proliferation by a means of pathways including the phosphoinositide 3-kinase [6], which prevents apoptosis, and the raf pathway which promotes cellular entry into G1 of the cell cycle [7].

Conversely, tumour suppressors are often activated to stimulate apoptosis or suppress proliferation as a stress response such as during DNA damage and oncogene activation; this ensures cell integrity is maintained and proliferation is kept under control. Loss of function to these genes promotes tumourigenesis. Typically for tumour suppressor genes to become inactivated loss of both alleles is necessary [8][9]. The transcription factor p53 is a

tumour suppressor gene mutated in over half of human cancers [10]. Mutations often occur in the DNA binding domain of p53 and thereby inhibit the transcription of important genes involved in cell cycle arrest, DNA repair processes, cellular differentiation and apoptosis [11].

1.2. Mitosis and the cell cycle

Figure 1.1 shows the cell cycle and the key checkpoints within it; on activation by DNA damage the G1/S phase checkpoint, the intra-S phase checkpoint and the G2/M phase checkpoint can impede S phase entry, S phase progression and mitotic entry respectively. Cyclin-dependent kinase (CDKs) activity is pivotal in regulating the cell cycle. The four main phases, G1, S, G2 and mitosis, are all positively controlled by cyclin-CDK complexes. Destruction of cyclins by the cell allows for the inactivation of CDKs and therefore differential cyclin levels permit the cycle to run smoothly. For example cyclin B-CDK activity promotes mitosis whilst preventing DNA replication. Once mitosis is complete cyclin B is broken down and its CDK activity is thereby reduced; this enables the cell to exit mitosis and permits DNA replication [12].

Mitosis is the final stage of the cell cycle which allows cells to divide into two identical daughter cells. This process, which involves the condensation of chromosomes and repression of gene expression, helps to minimise chances of damage to the hereditary genetic information to be passed on to daughter cells and ensure that the chromosomes carrying this information are divided equally [13][14].

Mitotic division is highly regulated by various checkpoints within the cell cycle which are only passed when the internal checking system at each stage is satisfied that cellular integrity has been maintained. These checkpoints ensure that DNA replication occurs only

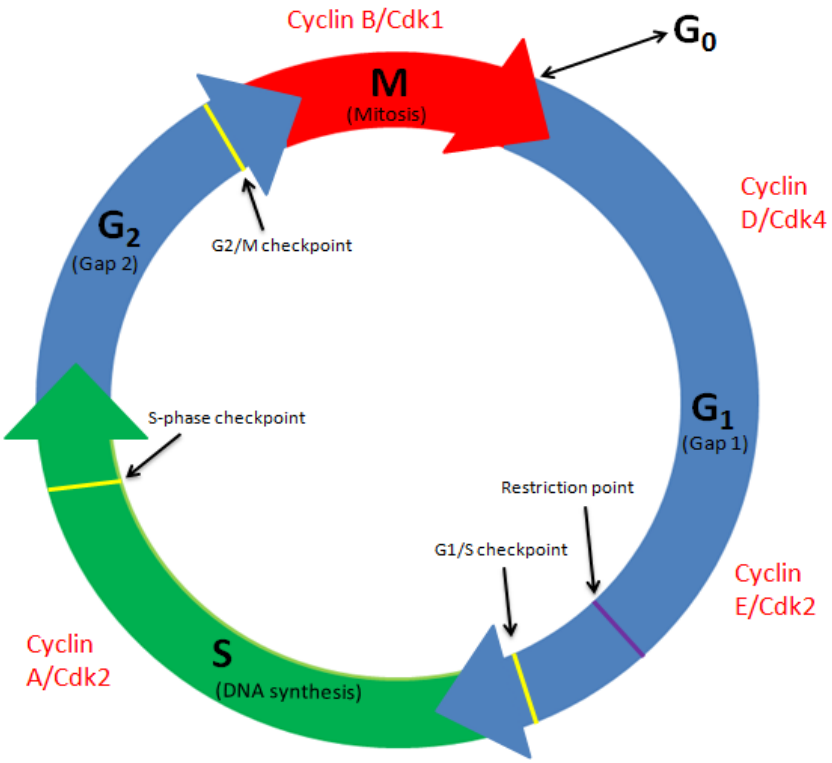

Figure 1.1 The cell cycle - A simplified diagram of the 4 main stages of the cell cycle (G1, S, G2 and M) with the corresponding checkpoints (Yellow bands) and G1 restriction point (Purple band) whereby cells become commited to another cycle of division. Key cell cycle regulatory cyclins and cdks are labelled in red.

once per cell cycle and is followed by cell division [15]. If at these checkpoints DNA damage is detected, cell growth and division is arrested and DNA repair processes are employed to correct the damage [16]. The fate of cells that are unable to be appropriately repaired is apoptosis; those that avoid this process, through oncogene activation or tumour suppressor gene inactivation may go on to divide in an uncontrolled manner.

The anaphase promoting complex, or cyclosome, (APC/C) allows for the readily interchangeable levels of CDK activity throughout the cell cycle. The APC/C is a cullin-RING finger E3 ubiquitin ligase and works by targeting cyclins for destruction, via ubiquitylation, by the 26S proteasome. Therefore both the timely activation and inactivation of APC/C appears crucial for efficient cell cycling [17][18].

Moreover, APC/C is regulated by the Spindle assembly checkpoint (SAC) proteins to ensure that cells do not exit mitosis prematurely. The SAC checks that all the chromosomes are attached to the microtubules of the mitotic apparatus; so that post division the chromosomes of each daughter cell are identical [19].

1.3. Ubiquitylation

Ubiquitylation is a key cellular process for targeted destruction of proteins. It is an essential process not only in the cell cycle but also for when proteins have been misfolded and removal is necessary to prevent potential cellular damage and endoplasmic reticulum (ER) stress [20]. The ATP dependent process, illustrated in figure 1.2, is carried out by three different enzymes, “ubiquitin activating enzyme” (E1), “ubiquitin-conjugating enzyme” (E2) and “ubiquitin ligase” (E3). Initially E1 binds to ubiquitin via a thio-ester bond; this subsequently enables ubiquitin to bind E2. E3 is then employed to facilitate the formation of an isopetide bond between the ubiquitin’s carboxy-terminus and the distinct

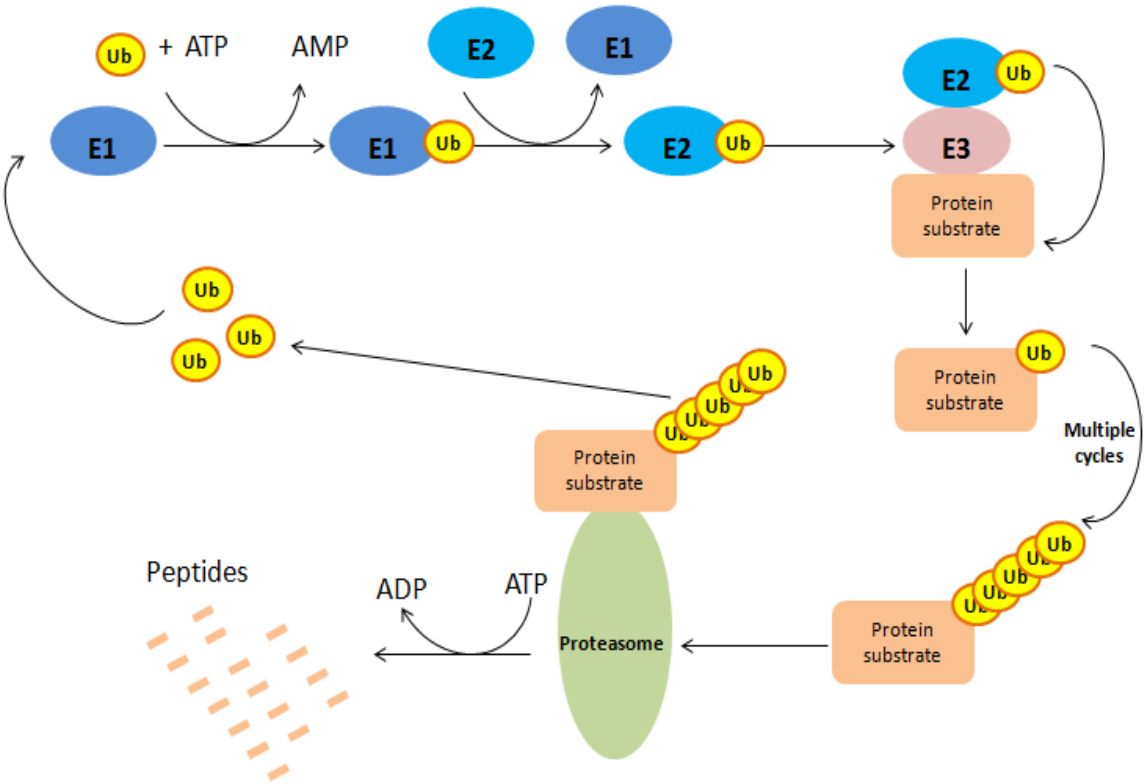

Figure 1.2. Ubiquitin proteasome pathway – An illustration of the ATP dependent ubiquitin (Ub) pathway. The enzymes E1, E2 and E3 interact and subsequently allow ubiquitination of protein substrate. After numerous cylces the protein is degraded into multiple peptide frangments by the proteasome and Ub is recycled [20].

lysine residues of the substrate protein. Many E3 ligases recognise only certain groups of substrate proteins, which may require post-translation modidications like phosphorylation, thus allowing process specificity. After multiple cycles of the ubiquitylation process the polyubiquitylated substrates are recognised by the 26S proteasome and subsequently degraded into small peptides. As this process contributes to the regulation of the cell cycle, abnormalities to the components of ubiquitin-dependent protein degradation may contribute to diseases such as cancer, yet components may alternatively provide novel therapeutic targets [21].

1.4. TRIM/RBBC proteins

The tripartite motif (TRIM) family of intracellular proteins are known for their role in ubiquitylation and have been shown to partake in many diverse cellular processes including DNA repair and antiviral immunity [22]. Currently, in humans and mice, over 70 proteins have been identified within this family which are characterised by their poorly conserved common N-terminal region comprising of a RING finger, B-boxes and a coiled coil domain (RBCC) collectively known as a TRIM domains [23].

The common structural features of TRIM proteins provide some functional similarities. For example, they are typically known for their ubiquitin ligase activity associated with their RING finger domain [24]. Additionally, the B-boxes and bromo domains are known chromatin interacting domains. These properties indicate that the proteins may play roles in both protein degradation and transcriptional regulation [22].

By genomic analysis, the TRIM protein family is typically divided into two distinct subgroups. Group 1 have a range of C-terminal domains which are highly conserved in vertebrates and also present in invertebrate species. In contrast, group 2 are characterised

by a common C-terminal SPRY domain; they are not present in invertebrates and are poorly conserved between mammals. As group 1 appears more evolutionary ancient it has been proposed that these proteins are important in the fundamental functioning of cells where as group 2 genes are more functionally diverse and may allow for novel functions of TRIM proteins in a species specific manner. These differences may allow biological responses between species to be targeted to their needs; for example in the control of viral infection and cell transformation [25].

Previous studies indicate that the ubiquitin ligase activity of some TRIM protein family members may be vital for regulating the degradation of tumour suppressors and oncogenic proteins. Mutations and altered expression levels of TRIM proteins have been identified in numerous human cancers supporting suggestions that their deregulation is involved in carcinogenesis [22]. In addition, it is notable that the RBCC motif of three TRIM proteins, namely transcriptional intermediary factor 1-alpha (TIF1α), promyelocytic leukemia (PML) protein and Ret finger protein (RFP), were found to form fusion oncoproteins with truncated derivatives of the proteins B-Raf, retinoic acid receptor-alpha (RARα) and ret respectively [26][27][28]. Together these findings therefore demonstrate a key role for the RBCC motif in cell transformation and cancer progression.

1.5. Transcriptional intermediary factor 1 family (TIF1)

The TIF1 family currently has four known members; TIF1α, β, γ and δ. Analysis of the TIF1 family members' amino acid sequences have indicated a role in chromatin-mediated regulation of transcription.

Previous studies, by Venturini et al., have shown that the TIF1 family members share a 25 amino acid TIF1 signature sequence (TSS). Removal of the TSS by deletional mutagenesis

prevents TIF1γ transcriptional inhibitory activity, indicating that this motif is involved in TIF1 dependent repression of transcription. This unique and conserved region between the TIF1 family proteins indicates that it exhibits a similar repressive function within TIF1α, β and δ [29].

Despite structural and functional similarities, TIF1 gene family members demonstrate a diverse array of actions. TIF1α (or TRIM24) acts to positively or negatively regulate the transcriptional activity of nuclear receptors by ligand-dependent interactions [28][30]. The importance of this transcriptional regulation has been previously demonstrated in TIF1α – null mice where lack of liver-specific tumour suppressor activity by TIF1α results in dysregulated cell cycle control in hepatocytes. This makes them more prone to genetic aberrations and consequently leads to the development of hepatocellular carcinoma [31]. TIF1β (TRIM 28) is part of the N-CoR1/HDAC3 histone deacetylase complex and has been shown to play a variety of roles including transcriptional repression of Krüppel-assocoiated box (KRAB) zinc-finger protein activity where its activity has been shown to be crucial in early stages of embryonic postimplantation development [32]. In addition, TIF1δ (TRIM66), which is predominantly expressed in elongating spermatids within the testis, interacts with heterochromatin protein 1 (HP1) and exhibits chromatin-mediated gene silencing during spermatogenesis [33].

1.6. TIF1γ and interacting proteins

TIF1γ was the third member of the TIF1 family to be identified and is otherwise known as TRIM33. Along with TIF1α and β, TIF1γ was seen to contain the highly conserved TSS within its central region (figure 1.3) [29]. TIF1γ is a nuclear protein expressed ubiquitously and similarly to the other TIF1 family members it displays transient transcriptionally repressive activity. Unlike TIF1α and β, TIF1γ does not appear to interact with the KRAB

domain of zing-finger transcription factors or with HP1 and it also displays no nuclear receptor activity. TIF1γ did however demonstrate that when tethered to a promoter it does have silencing action; these findings indicate that TIFγ uses alternative binding partners to repress transcription [29].

Figure 1.3. TIF1γ structure – A linear representation of the conserved TIF1γ structural domains including; the RING finger, B-boxes, coiled coil, TSS, PHD and Bromo domain.

TIF1γ was first shown to be associated with paediatric thyroid cancer, where on fusion with the RET receptor tyrosine kinase, it is seen to stimulate aberrant tyrosine kinase activity [34]. TIF1γ has since been associated with other diseases such as chronic myelomonocytic leukaemia (CMML) where its tumour suppressive actions are down regulated through hypermethylation of its gene promoter [35]. It has also been linked to pancreatic ductal adenocarcinoma (PDAC) where it works in collaboration with the v-Ki-ras2 Kirsten rat sarcoma viral oncogene homolog (KRAS) to induce pancreatic tumour development [36].

In contrast to its actions as a repressor of gene transcription, studies have also proposed it exhibits de-repressor activity. Studies have shown that TIF1γ may interact with TIF1α to form a hetero-oligomer and this oligomerisation may work as an alternative transcriptional regulatory mechanism by which TIF1γ can relieve the repressive actions of TIF1α [37].

Previous studies have also indicated a role for TIF1γ in haematopoietic, mesenchymal and epithelial cell differentiation. The studies show that the TGF-β-dependent differentiation process may require TIF1γ to compete with SMAD4 to bind to the active transcriptional complexes SMAD2/SMAD3. However some studies suggest TIF1γ acts as a monoubiquitin ligase of SMAD4 and dissociates the SMAD2/3-SMAD4 complexes thereby inhibiting TGF-β signalling [38]. Recent work in the Turnell laboratory identified TIF1γ as a binding partner of APC/C and, through specific binding to APC3 and Cdc20, it modulates the progression of the cell cycle through mitosis [39]. The role of TIF1γ in regulating the cell cycle is of particular interest as further understanding of cell cycle regulation is necessary to establish the importance of different proteins and complexes in the normal functioning of the cell cycle.

Although previous studies indicate a variety of roles for TIF1γ, the specific functioning of TIF1γ is yet to be fully understood. A better understanding of TIF1γ interactions and activity may provide novel molecular targets for associated diseases such as cancer.

1.7. Hypothesis and Aims

We hypothesise that TIF1γ is post translationally modified by phosphorylation during mitosis by interacting proteins. This modification might be important for cell cycle progression as TIF1γ exhibits tumour suppressor activity and allows for progression through mitosis.

To further understand the role of TIF1γ in mitosis the aims of this project were:

1) To determine differential binding proteins of TIF1γ at different stages of the cell cycle.

2) To identify key phosphorylation sites of TIF1γ and examine phosphorylation changes to TIF1γ at different stages of the cell cycle.

2. Methods

2.1. Cell maintenance and subculture

The HeLa cell line was used in this study, it is a cervical carcinoma cell line characterised by the expression of human papilloma virus (HPV-18). The cell line was acquired from ATCC (product number CCL-2.2).

Sterilised reagents were all acquired from Invitrogen and stored at 4°C, unless noted otherwise. Prior to use reagents were prewarmed to 37°C unless stated otherwise. The cell culture medium Dulbecco's Modified Eagle's Medium (DMEM) was supplemented with 2mM L-glutamine and 8% v/v foetal calf serum (FCS) before use.

Cells were grown in DMEM and incubated at 37°C in 95% air, 5% carbon dioxide. For cell subculture of confluent cells medium was removed and cells were washed twice in PBS. Then trypsin solution was added (1ml) and cells were incubated at 37°C for 5 minutes or until cells had detached from the surface. Trypsin was inactivated by the addition of DMEM; cells were pelleted by centrifugation at 1500rpm for 5 minutes. The media was removed; cells were resuspended in fresh DMEM and plated at the appropriate dilution.

2.2. DNA damage

Cells were either treated by UV exposure for 30 seconds at 10J/m² or the addition of 1mM hydroxyurea for the appropriate time. Cells were then washed twice in saline and harvested in lysis buffer (9M urea, 50mM Tris (pH 7.4) and 0.15M β-mercaptoethanol).

2.3. Mitotic arrest

Cells at 90% confluency were incubated at 37°C overnight in DMEM further supplemented with 400ng/ml of nocodazole. Mitotic cells were harvested by shake off.

2.4. Nocodazole release

DMEM containing nocodazole from the mitotic arrested cells was removed and fresh DMEM medium was added to the cells.

2.5. Cell transfection

cDNA was acquired from Dr Caroline Hill (LRI) [40] for different TIF1γ domains, flag tagged TIF1γ wild type (WT), TIF1γ ΔTRIM, TIF1γ ΔRING and TIF1γ ΔPHD/Bromo domain. 4µg of DNA/ 8µl of lipofectamine 2000 (Invitrogen) was used and the transfection was completed following manufacturer's instructions; cells were incubated for 6 hours and then media was replaced with fresh DMEM.

2.6. Immunoblotting

Antibody	Dilution	Secondary antibody used (DAKO)	Blocking agent	Supplier
TIF1 γ	1:2000	Anti-rabbit (1:3000)	Milk	Turnell
Geminin	1:250	Anti-protein G (1:1000)	Milk	Sigma
Cdt1	1:500	Anti-protein G (1:1000	Milk	Sigma
Chk1	1:1000	Anti-mouse (1:2000)	Milk	Sigma
B-actin	1:2000	Anti-mouse (1:2000)	Milk	Sigma
pChk1 (5317)	1:3000	Anti-rabbit (1:3000)	BSA	Bethyl
Cyclin B1	1:1000	Anti-mouse (1:2000)	Milk	Sigma
Flag	1:3000	*Conjugated	Milk	Sigma
APC 7	1:2000	Anti-rabbit (1:3000)	Milk	Sigma

Table 2.1: Primary and secondary antibodies

Cells were washed twice in saline and harvested in lysis buffer (9M urea, 50mM Tris (pH 7.4) and 0.15M β-mercaptoethanol). After a 10 minute lysis buffer incubation cells were detached from the dish surface using a scraper. Cells were then sonicated for 10-15 seconds and centrifuged for 20 minutes at 13000rpm.

The protein concentration was then determined by adding 5ul of the sample to 1ml of Bradford reagent (Bio-Rad) and incubated at room temperature (RT) for 10 minutes. The absorbance was read at λ 595nm and concentration determined from a bovine serum albumin (BSA) standard curve of known concentrations (0-30µg).

50µg/ml of each protein sample was added to new Eppendorf tubes and equal quantities of sample buffer (1 unit of 10% w/v SDS to 2 units of 9M urea in 50mM Tris (pH 7.4)) plus 5% v/v β-mercaptoethanol was added, in a 1:1 ratio of the largest volume, to each sample. Samples were mixed and boiled for 5 minutes at 90°C on a heating block and then centrifuged briefly at 13000rpm.

Sodium dodecyl sulphate-polyacrylaminde gel electrophoresis (SDS-PAGE) was used to separate the protein samples by molecular weight. 10% w/v acrylamide gel (from 40% acrylamide stock, 0.1M Tris, 0.1M bicine (N,N-bis(2-hydroxyethyl)glycine), 0.1% w/v SDS, 0.25% TEMED (N,N,N',N'-tetramethylethylenediamine) and, added last, 0.06% ammonium persulphate (APS)) was mixed and poured into electrophoresis apparatus, with a comb placed into the top to form wells, and left to polymerise. Then, on removal of the comb, wells were washed and filled with running buffer (0.1M Tris (pH 7.4), 0.1M bicine, 0.1% w/v SDS). Wells were loaded individually with 50µg of protein samples or a protein ladder used to estimate the size of bands once the gel is run. Once loaded the apparatus lid

was placed on and filled with running buffer and the gels were then electrophoresed overnight at 10mA per gel.

Proteins were transferred from the gel onto nitrocellulose paper (PALL) using a transfer cassette placed in Hoefer transblot electrophoresis apparatus with transfer buffer (192mM glycine, 25mMTris and 20% v/v methanol) at 250mA for 6 hours. The nitrocellulose membrane was then removed and successful transfer was assessed by washing with 1% w/v Ponceau S red stain (Sigma) (in 3% w/v trichloroacetic acid (Sigma)) for a few minutes. The membrane was destained by rinsing with water and washing with Tris-buffered saline with Tween 20 (TBS-T) (0.1% v/v Tween™ 20, 0.2M sodium chloride (NaCl) and 0.02M Tris (pH 7.6)) on an orbital shaker. Blots were washed with appropriate blocking agent (5% w/v skimmed powered milk or 5% w/v BSA in TBS-T) for 45 minutes and then rinsed with TBS-T. Blots were placed in bags and sealed with primary antibodies and left at 4°C on a shaker overnight. Then blots were washed in TBS-T on the orbital shaker for 15mins and placed in new sealed bags with secondary antibody and left at RT for 2 hours on the shaker. Blots were washed for 15 minutes 3 times on the orbital shaker.

Blots were drained and 5ml of both Immobolin western substrate reagent and HRP-enzyme luminal reagent (Millipore) was added and left for 1 minute at RT. Blots were wrapped in Saran film and placed in a developing cassette. In the darkroom blue x-ray film (Wolt laboratories) was placed onto the blots and the cassette was closed for the required amount of time to get the desirable exposure. Film was then placed into the xograph developer.

2.7. Immunoprecipitation

Cell lysates and reagents were kept on ice unless stated otherwise. Cells were harvested, the same as for the western in 1ml of the chosen lysis buffers (stated in the results section;

either HiLo (50mM Tris (pH 7.4), 0.825M NaCl, 1% v/v NP-40) or NETN (50mM Tris (pH 7.4) 1mM EDTA (pH 8.0) 1% v/v NP-40, 200mM NaCl)). For HiLo cells were sonicated for 10-15 seconds and for NETN cells were homogenised with a dounce homogeniser. Lysates were then centrifuged for 20 minutes at 15000rpm and using a needle the supernatant was removed, avoiding the top lipid layer, and placed into a new falcon tube. Total lysates for each batch were split into Ependorfs equally and immunoprecipitated overnight, on a spinning wheel at 4°C, with the appropriate antibody. Next, 20µl of packed Protein G-sepharose beads (KCL) were added at a 1:1 ratio with lysis buffer, and samples were place back on the spinner at 4°C for 3 hours. The samples were then spun at 4°C and washed 4-6 times in the respective lysis buffer. Sample buffer was added; samples were boiled for 5 minutes, loaded on to gel and blotted the same as described in the western.

Lysis buffer	Contents
NETN	50mM Tris (pH 7.4) 1mM EDTA (pH 8.0) 1% v/v NP-40, 200mM NaCl
HiLo	50mM Tris (pH 7.4), 0.825M NaCl, 1% v/v NP-40
Lysis buffer	9M urea, 50mM Tris pH 7.4 and 0.15M β-mercaptoethanol

Table 2.2: Cell lysis buffers

2.8. Phosphatase treatment of Immunoprecipitates

Immunoprecipitation is carried out as described but after washing samples post incubation with Protein G sepharose beads samples were incubated for one hour in 200units λphosphatase in 25µl of buffer (1:1 $MnCl_2$: phosphatise buffer) (Sigma).

2.9. Site directed mutagenesis

To mutate phosphorylation sites of TIF1γ PCR was employed to make cDNA for transformation. Table 2.3. shows the site directed mutagenesis master mix used (QuikChange, Agilent, UK). On ice, primer was added (1µg/ml of master mix).

Reagent	Amount per sample
Oligo Forward (250ng)	2.5µl
Oligo Reverse (250ng)	2.5µl
Plasmid (100ng)	1µl
10 x reaction buffer	5µl
dNTP (10mM)	1µl
Nuclease free water (NFW)	37.5µl
Pfu DNA polymerase (2.5U/µl)	0.75µl

Table 2.3: Site mutagenesis mastermix used per sample

Primers used (from Dr Caroline Hill, LRI) [40]:

5' gc ctt gtt aat gga aag gcc cca att cga agc ctc 3' ala (Forward)

5' gag gct tcg aat tgg ggc ctt tcc att aac aag gc 3' ala (Reverse)

Samples were prepared on ice and then placed in the a thermal cycler with the following settings;

95°C – 30 sec } **x 1 cycle**
95°C – 30 sec
55°C – 1 min } **x 18 cycles**
72°C – 18 min
72°C – 5 min } **x 1 cycle**
4°C – indefinitely

1µl of restriction enzyme Dpn1 (20U/PCR) was added to the PCR mix and incubated at 37°C for 3 hours. 20µl of bacterial strain XL10 Gold (Agilent, UK) plus 0.89µl of β-mercaptoethanol was incubated on ice for 10 minutes and then 4µl of PCR mix was added and left to incubate on ice for 30 minutes. The bacteria cells were then heat shocked for 2 minutes at 42°C and recovered on ice for 5 minutes. 0.5ml of NZY+ broth was added and samples were left in a shaking incubator at 37°C for 1 hour. Samples were plated out on Luria broth (LB) agar plates (with 100µg/ml ampicillin, 1.5% agar) overnight. Plates were checked for colonies and if non found mutagenesis was repeated altering protocol (e.g. change bacterial strain, PCR cycles or primer concentration).

2.10. Mass spectrometry (MS)

Cells were harvested in NETN buffer on ice and immunoprecipitated with TIF1γ antibody and protein G beads, as previously described. The beads were washed 4 times in NETN buffer and twice in detergent free buffer. 0.5ml of 9M urea, 50mM ammonium bicarbonate (ABC) was added to denature the beads and vortexed regularly at RT for 1 hour. Beads were spun down at 15000rpm and supernatant containing protein was collected. 50mM of dithiothreitol (DTT) (final concentration) was added for 30 minutes at 56°C followed by 100mM iodoacetamide (final concentration) for 30 minutes in the dark at RT. Supernatant was added to FASP (filter aided sample preparation) filters and centrifuged at full speed until all has flowed through. Flow through was discarded and filters were washed 4 times with 50mM ABC. FASP filters were placed in new tubes and 1µg of trypsin (in 200µl of resuspension buffer), per IP, was diluted in 50mM ABC to give final volume of 300µl. This was added to filters and left overnight at 37°C. Samples were centrifuged at full speed to collect tryptic peptides, transferred to low binding Ependorfs, washed with 50mM ABC, centrifuged and flow through was collected. Samples were dried

down in a vacuum centrifuge and resuspended and mixed in 40µl of water with 1% acetonitrile (AcN) and 1% formic acid (FA). 10µl was loaded onto the MaXis impact (Bruker) mass spectrometer.

For phospho-purification of samples, prior to drying the samples down, additional preparation was employed. 1mg/MS sample of Titansphere TiO_2 beads were added to binding buffer BB (80% AcN, 1% trifluoroacetic acid (TFA) and 1M glycolic acid) and left to swell for 10 minutes. The beads were centrifuged and supernatant discarded and washed in BB rotating for 10 minutes and supernatant was then removed. 100µl of BB was added to the beads and peptides were resuspended in 900µl of BB. Peptides were added to the beads and left rotating at RT for 20 minutes.

Samples were washed 4 times in BB, by centrifugation of beads and discarding supernatant, and once in a final wash buffer of 80% AcN and 0.1% TFA. 100µl of eluting buffer was added (400mM ammonium hydroxide) and vortexed occasionally for 10 minutes at RT. Supernatant was collected and samples were dried down and preparation for MS was completed as before.

3. Results

Previous results from the Turnell lab have suggested that TIF1γ is post-translationally modified during mitosis [39].Therefore in this investigation we initially wanted to confirm this previous finding and determine whether TIF1γ was modified by phosphorylation. From this we would like to establish the site at which TIF1γ is post-translationally modified during mitosis and identify potential TIF1γ interacting proteins which may be involved.

3.1. TIF1γ and cyclin B1 phosphorylation during nocodazole release

Initially we aimed to confirm previous results which suggested TIF1γ may be phosphorylated during mitosis. To do this we used nocodazole to arrest cells in mitosis. This was followed by nocodazole release and cells were harvested over a time course of 0, 0.5, 1, 2 and 4 hours post release to analyse cells as they progress through the cell cycle. We blotted for TIF1γ and cyclin B1, a known mitotic regulator controlled by phosphorylation, and identified changes in the mobility of both proteins through SDS-PAGE seen in figure 3.1. The results show that during mitotic arrest (0 hours post release) mobility on the gel of TIF1γ is reduced but after 0.5 hours, once the cells have begun to progress through the cell cycle, the mobility increases again. Additionally the results show that protein expression levels for cyclin B1 change through the cell cycle with levels initially increasing on nocodazole release and after 4 hours levels appear to decrease considerably. The changes in cyclin B1 levels were used to indicate cell cycle status throughout the 4 hour time course, Cyclin B1 levels are high at the start of mitosis, with levels reducing as cells progress through mitosis and then levels become minimal in G1. Overall these results suggest that TIF1γ is post translationally modified during mitosis.

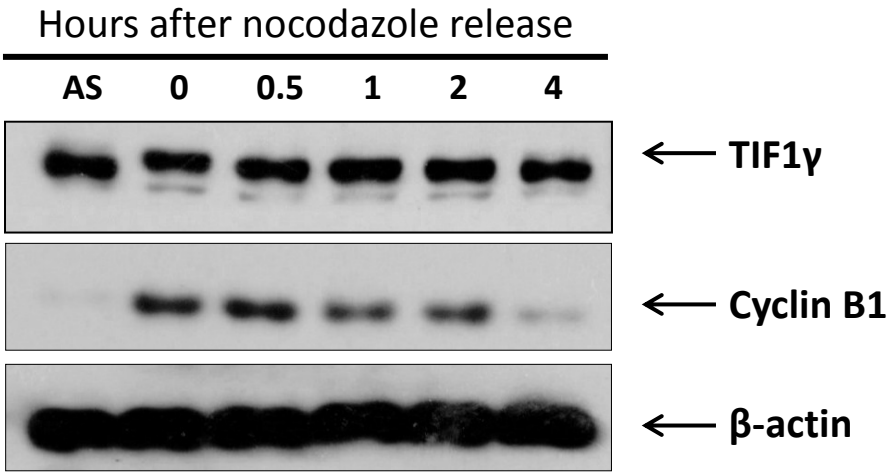

Figure 3.1. TIF1γ mobility on SDS-PAGE following nocodazole treatment and nocodazole release - HeLa cells were either left untreated (AS) or treated with nocodazole to induce mitotic arrest and harvested in lysis buffer at the indicated times after nocodazole release. Western blotting was used for TIF1γ to examine changes to protein mobility, Cyclin B1 to indicate the stage of the cycle and β-actin as a loading control.

3.2. DNA damage induction by ultra violet (UV) light and hydroxyurea (HU) treatment

To establish whether DNA damage could also induce post translational modifications of TIF1γ and DNA damage associated proteins Chk1 and pChk1 we treated cells to either UV light or HU treatment to inflict DNA damage. The cells were harvested over a time course of 0, 0.5, 1, 2 3, 4 and 6 hours to detect changes over time in response to DNA damage. Immunoblot analysis of the proteins showed that mobility of TIF1γ was unchanged after both UV and HU treatment suggesting that no post translation modifications were induced by DNA damage over the studied time course (figure 3.2). The Chk1 antibody was used as

a loading control and protein levels appeared constant throughout. However, when using a phosho-specific antibody (pChk1), the immunoblot shows increased phosphorylation levels of Chk1 indicating that a DNA damage response pathway is activated following UV and HU treatment.

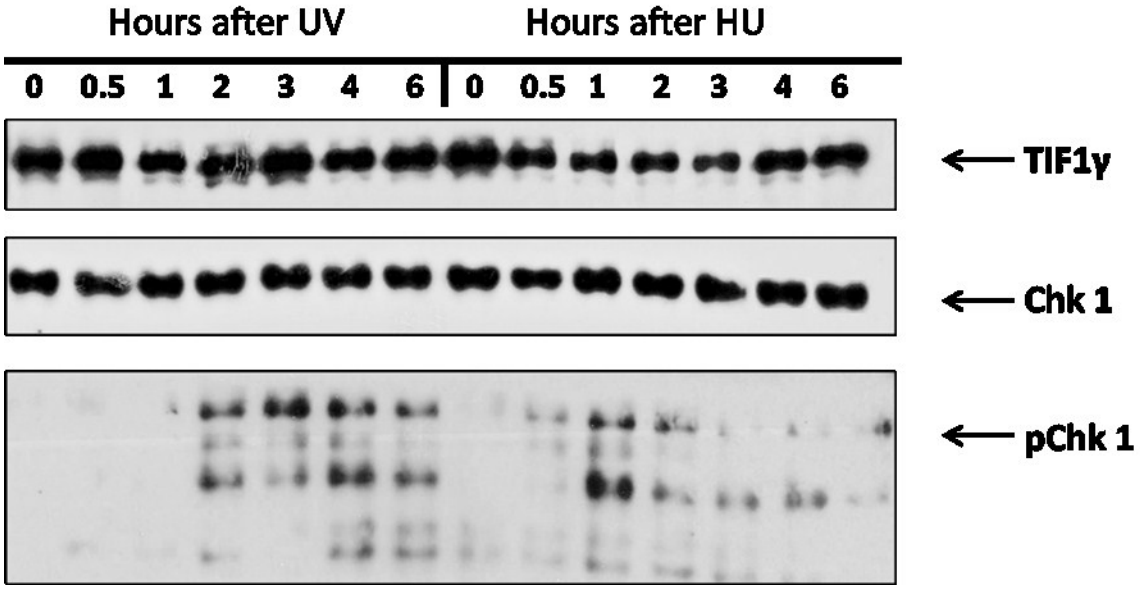

Figure 3.2. TIF1γ mobility, Chk1 and pChk 1 expression after HU and UV treatment
HeLa cells were subjected to either UV or HU treatment to induce DNA damage. Cells were harvested in lysis buffer at the times indicated post treatment and examined by western blotting for TIF1γ to detect changes in SDS-PAGE mobility and for pChk1 to assess expression levels. Chk1 was used as a loading control.

3.3. TIF1γ immunoprecipitation(IP) with λphosphatase treatment

As previous analyses suggest that TIF1γ is post translationally modified in mitosis we wanted to determine whether this was a phosphorylation modification. Therefore we treated immunoprecipitates, of cells in mitotic arrest post nocodazole treatment, with λphosphatase. Immunoblotting of TIF1γ showed an increase in mobility of TIF1γ on SDS-PAGE following λphosphotase treatment (figure 3.3); as λphosphatase is an enzyme known to dephosphorylate proteins, these data suggest that TIF1γ is phosphorylated during mitosis.

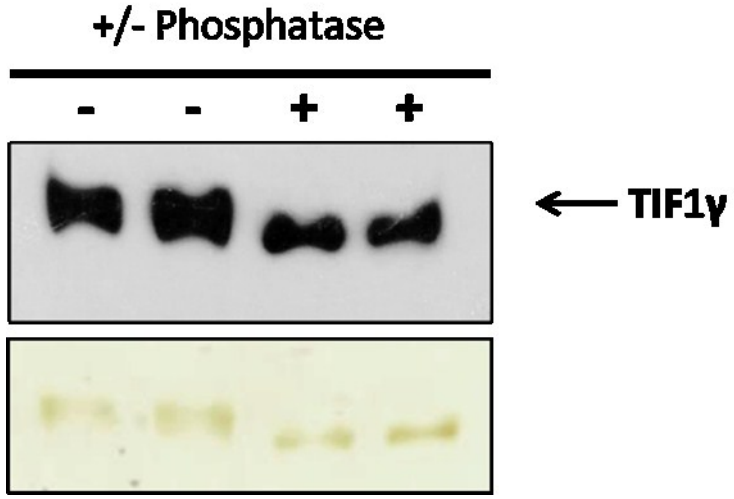

Figure 3.3. TIF1γ mobility on SDS-PAGE following λ-phosphatase treatment
HeLa cells were treated with nocodazole to induce mitotic arrest and harvested in HiLo buffer. Cells were either left untreated (-) or treated with λ-phosphatase (+). Changes to protein mobility on SDS-PAGE were assessed by western blotting for TIF1γ. The upper image is of TIF1γ exposure on x-ray film and the lower image shows TIF1γ directly on the nitrocellulose membrane (to show a sharper image).

3.4. Phosphorylation site identification by cDNA transfection of asynchronous and mitotic arrested cells

As the previous analyses indicated that the shift in TIF1γ mobility during mitosis is a result of TIF1γ phosphorylation we wanted to determine which domain of TIF1γ was phosphorylated. This was achieved by expressing cells with cDNA which lacked specific domains of TIF1γ in asynchronous cells and determining changes to mobility following mitotic arrest. In theory, if the domain which holds the mitotic phosphorylation site is missing then TIF1γ will not be phosphorylated during mitosis and no change in mobility will be seen between asynchronous and mitotic cells. Cells were therefore transfected with FLAG-tagged WT, ΔRing, ΔTrim and ΔPHD-Bromo domains of TIF1γ. After 24 hours half of the cell population were treated with nocodazole to induce mitotic arrest whilst the other half remained untreated. Cells were harvested in HiLo buffer and samples were measured for protein levels and separated by SDS-PAGE. From the western blot analysis it can be concluded that there was a change in TIF1γ mobility on SDS-PAGE between asynchronous and mitotic lysates transfected with WT, ΔRing and ΔTrim domains. Yet little change to the mobility of TIF1γ following ΔPHD-Bromo transfection was seen between the two cell populations. This suggests that the PHD-Bromo domain holds the mitotic phosphorylation site (figure 3.4.A).

Additionally, to study further whether the mitotic phospho-site resides within the TIF1γ PHD-Bromo domain, as before we transfected asynchronous cells with cDNA, this time to express FLAG-tagged TIF1γ Trim and PHD-Bromo domains, and again half the cell population was treated with nocodazole. Here, the immune blotting results show no obvious change to protein mobility between asynchronous and mitotic cells expressing either of the TIF1γ Trim or PHD-Bromo domains (Figure 3.4.B). The results oppose those

of the previous experiment as we would have expected the PHD-Bromo domain to be phosphorylated during mitosis. Considerations for these results have been made in the discussion.

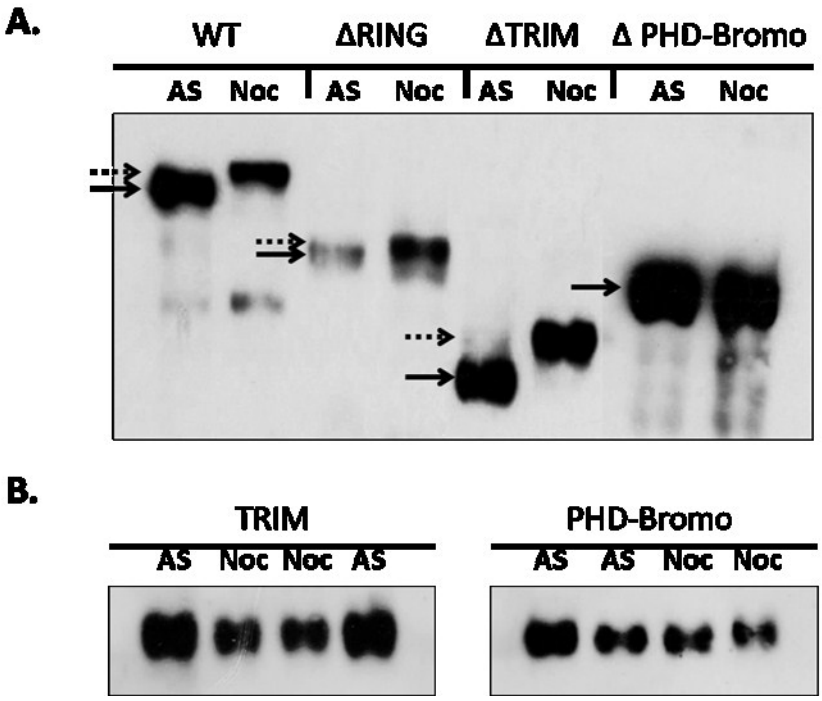

Figure 3.4. Mobility of mutated TIF1γ domains on SDS-PAGE following mitotic arrest – HeLa cells were transfected with cDNA expressing the indicated FLAG-tagged TIF1γ Wt or mutant domains. (A) shows TIF1γ WT, ΔRING, ΔTRIM and ΔPHD-Bromo domains and (B) shows TIF1γ TRIM and PHD-Bromo domains. Cells were either left untreated (AS) or subjected to nocodazole treatment (Noc) to induce mitotic arrest and then harvested in HiLo buffer. Western blotting for FLAG was employed to determine the mobility of the TIF1γ derivatives following mitotic arrest. (The arrows in 'A' point to the centre of the protein bands for each mutant domain, with solid arrows showing the mobility of unmodified proteins and dashed arrows indicating the upwards shift in mobility of proteins that have been modified).

3.5. Mass spectrometry (MS) for identification of TIF1γ phosphorylation sites and interacting proteins

To identify TIF1γ interacting proteins in both asynchronous and mitotic cell populations we employed MS. Both cell populations were harvested in NETN buffer and interacting proteins were immunoprecipitated overnight with anti-TIF1γ, IPs then were isolated using Protein G beads and prepared using FASP filters followed by trypsinisation before loading on to the MS machine. The MS results in table 3.5 show the proteins found to interact with TIF1γ in the asynchronous and mitotic samples. Interestingly these analyses reveal that Cdt1 and Geminin interact with TIF1γ in both the asynchronous and mitotic samples; figure 3.5.1 shows the MS/MS spectra for Geminin and Cdt1. These proteins were picked out from the others in table 3.5 as they are known to regulate the cell cycle, particularly DNA replication [41], and therefore interaction with TIF1γ may suggest an undiscovered role for TIF1γ at this stage of the cell cycle.

Protein	Function	MW	Number of peptides	Sequence coverage (%)	Mascot score
Asynchronous					
TIF1γ	E3 ubiquitin-protein ligase	122.4	43	34	1451.2
LMP	Bone formation/ may act as a scaffold for the assembly of proteins	49.8	10	30.6	385.9
TRIM21/SS-A	E3 ubiquitin-protein ligase	54.1	6	12.2	259.4
Cdt1	DNA replication factor	60.4	5	7.9	174.8
TIF1α	Transcriptional coactivator and E3 ubiquitin-protein ligase activity	116.8	4	3.6	114
ATP synthase subunit α	ATP synthesis from ADP	59.7	2	3.1	95.3
POTE-2	ATP binding	121.3	3	2.4	88
Geminin	Inhibitor of DNA replication	23.6	2	16.3	81.8
S100-A8	Inflammation and immune response regulation	10.8	1	11.8	62.4
Tubulin-β-IIa	The main component of microtubules	49.9	1	2.7	32.7
Nocodazole					
TIF1γ	E3 ubiquitin-protein ligase	122.4	28	23.4	743.7
TRIM21/SS-A	E3 ubiquitin-protein ligase	54.1	7	14.3	214.2
LMP	Bone formation/ may act as a scaffold for the assembly of proteins	49.8	5	12.3	211.8
TIF1α	Transcription intermediary factor 1-alpha OS=Homo sapiens GN=TRIM24 PE=1 SV=3	116.8	4	3.1	96.6
Geminin	Inhibitor of DNA replication	23.6	1	6.2	85.8
Cdt1	DNA replication factor	60.4	3	4.2	47.8
ATP synthase subunit α	ATP synthesis from ADP	59.7	1	2	39.2

Table 3.5. The TIF1γ-interacting proteins identified by mass spectrometry

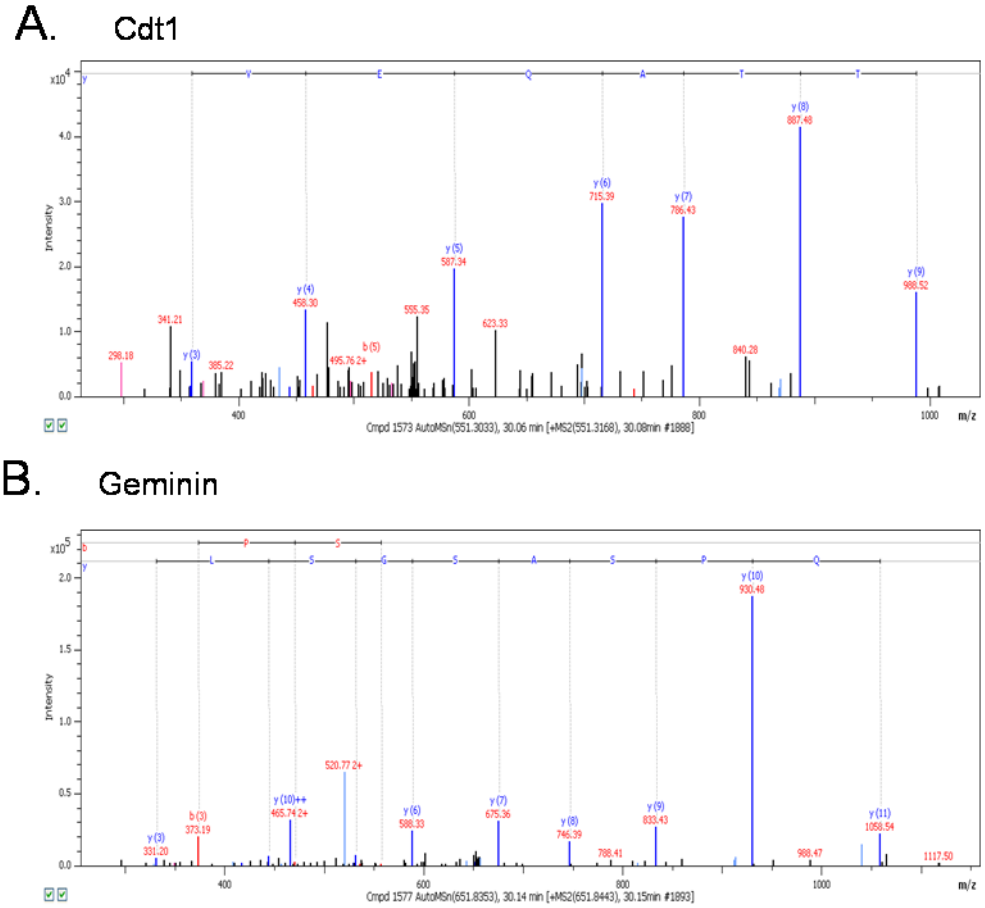

Figure 3.5.1. **<u>Mass spectromic identification of TIF1γ-interacting peptides from mitotic TIF1γ immunoprecipitates</u>** - (A) shows the ions generated by MS/MS of the Cdt1 peptide LTTAQEVLAR and (B) shows the ions generated by MS/MS of the Geminin peptide MIQPSASGSLVGR

Following our results suggesting TIF1γ is phosphorylated during mitosis we also used MS to identify TIF1γ phosphorylation sites. This enabled highly sensitive identification of phospho-purificated proteins to locate potential sites of phosphorylation. Asynchronous and mitotic samples were prepared as before, the peptides were then phospho-purified and run on the MS. The MS/MS results show that TIF1γ is phosphorylated at serine (S)856, S862 and S1119 (of the PHD-Bromo domain) during mitosis (figure 3.5.2.) and at S862 and S1119 in asynchronous cells. This suggests that the phosphorylation, seen in our previous analyses during mitosis, may occur at the S856 site.

To further investigate the importance of the phosphorylation sites identified by the MS we aimed to use site directed mutagenesis. By mutating the phosphorylation sites that we identified by MS, and subsequently assessing the effects of eliminating the site, we could establish whether these specific post translation modifications to TIF1γ play an essential role in its functioning. Unfortunately, despite repeating numerous times with alternative bacterial strains and increasing the PCR cycle number, we did not manage to isolate any colonies to screen for successful mutagenesis.

In addition, the MS results identified phosphorylation of S391 and threonine (T)262 of Cdt1 in the mitotic cells but not in the asynchronous (figure 3.5.3). This post translational modification may therefore contribute to the regulation of Cdt1 and thus DNA replication.

A. S856

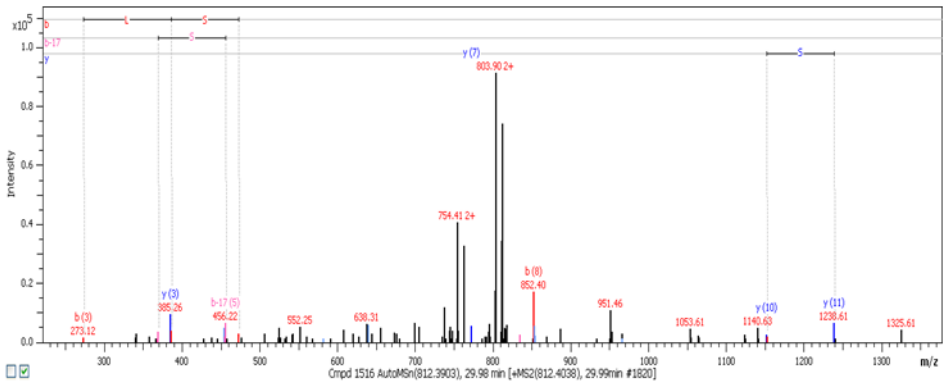

B. S862

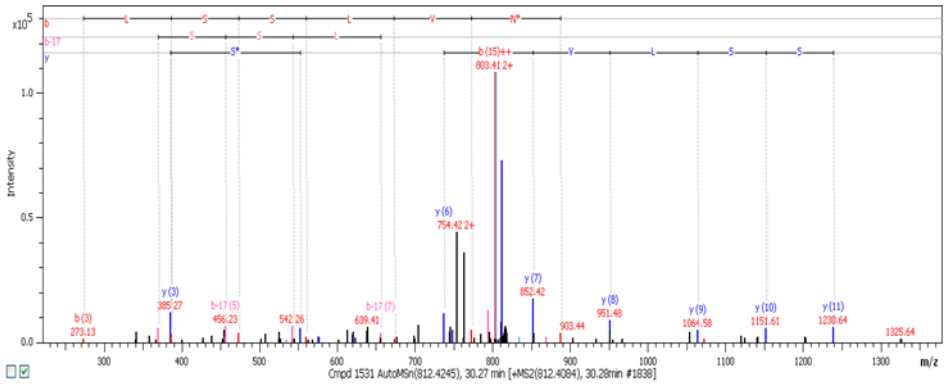

C. S1119

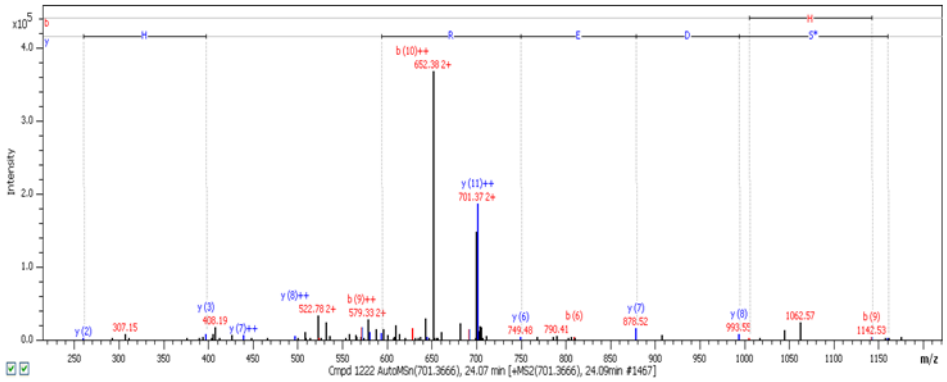

Figure 3.5.2. Mass spectromic identification of phospho-TIF1γ peptides from mitotic TIF1γ immunoprecipitates- (A) shows the ions generated by MS/MS of the phospho-TIF1γ peptide QSGLSSLVNGKSPIR (B) shows the ions generated by MS/MS of the phospho-TIF1γ peptide QSGLSSLVNGKSPIR and (C) shows the ions generated by MS/MS of the phospho-TIF1γ peptide LKSDERPVHIK.

A. S391

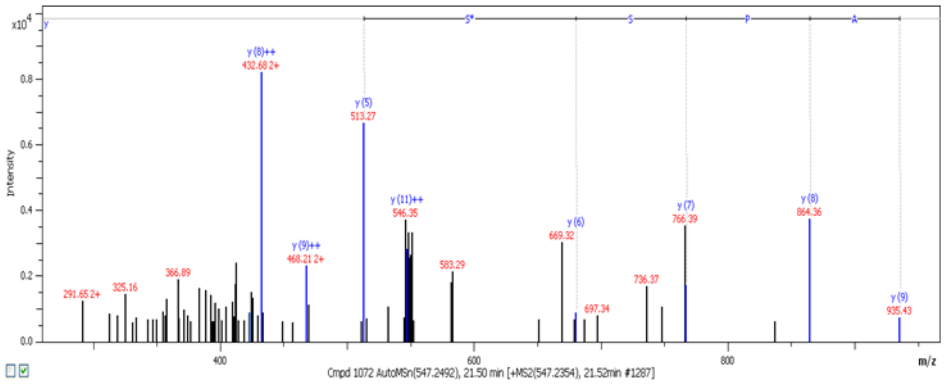

B. T262

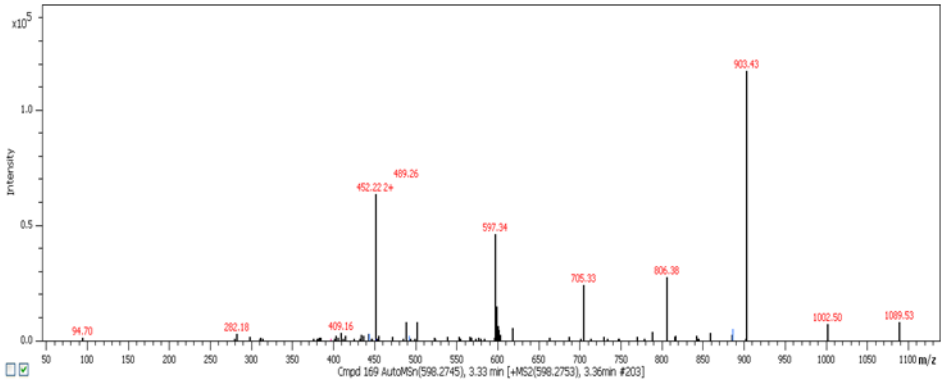

Figure 3.5.3. Mass spectromic identification of TIF1γ-interacting phospho-peptides from mitotic TIF1γ immunoprecipitates- (A) shows the ions generated by MS/MS of the phospho-Cdt1 peptide SAAPSSPGSPR and (B) shows the ions generated by MS/MS of the phospho-Cdt1 peptide QERSVPTFKDGTR

3.6. Geminin and Cdt1 IP with TIF1γ

As the proteins Geminin and Cdt1 have been previously seen to play a role within cell cycle control we found their interaction with TIF1γ of particular interest. Subsequently, In order to validate the MS results showing that both Geminin and Cdt1 bind to TIF1γ, a series of IPs were performed. Firstly we immunoprecipitated TIF1γ in asynchronous cells, and subsequently performed a western blot using Geminin and Cdt1 antibodies to see if they IP with TIF1γ and then, in reverse, TIF1γ was immunoblotted to determine whether it IP with Geminin or Cdt1. From the results in figure 3.6.1. we can see that Geminin and Cdt1 did IP with TIF1γ which validates the results from MS. However, TIF1γ did not IP with either Cdt1 or Geminin when we did the IP in reverse.

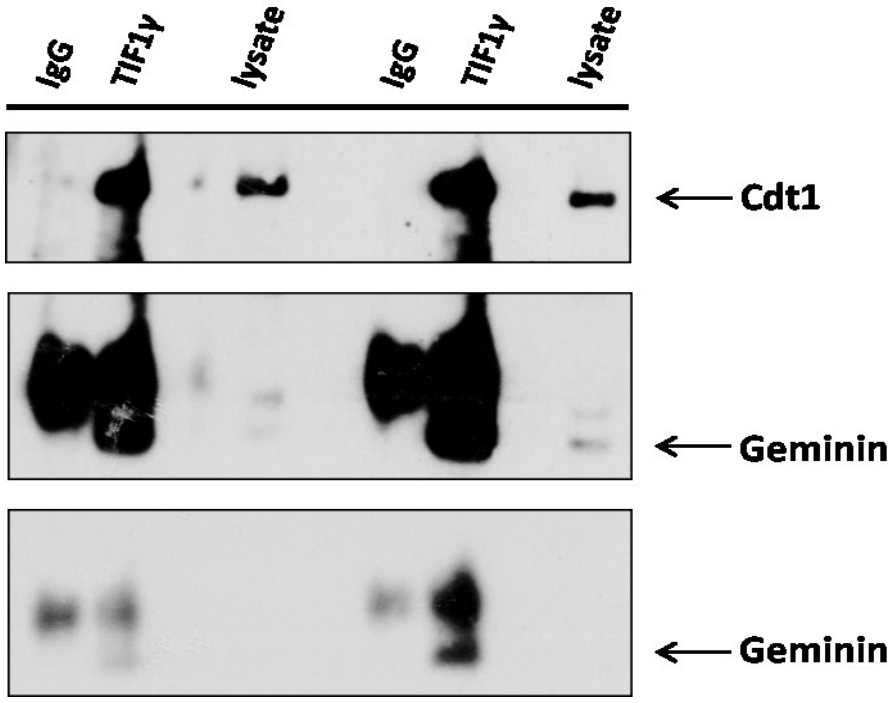

Figure 3.6.1. Immunoblot of TIF1γ-interacting proteins Cdt1 and Geminin from asynchronous TIF1γ immunprecipitates -HeLa cells were harvested in NETN lysis buffer and TIF1γ was immunoprecipitated with bound proteins which were then incubated with Protein G-sepharose beads and later eluted. Eluted proteins run on SDS-PAGE were examined by western blotting for the presence of, the TIF1γ interacting proteins of interest, Geminin and Cdt1.

As we found that Cdt1 and Geminin IP with TIF1γ in asynchronous cells we decided to repeat the IP with both asynchronous and nocodazole-arrested cells to investigate whether the proteins also interact with TIF1γ during mitosis. The immunoblot verifies the MS results and shows that TIF1γ interacts with Cdt1 and Geminin in both asynchronous and mitotic cells (figure 3.6.2). However, in figure 3.6.2, we can see that the mobility of Cdt1 on SDS-PAGE in the mitotic cells is reduced. This shift indicates that Cdt1 is post translationally modified in mitosis; supporting the previous MS results which identified two phosphorylation sites in the mitotic samples. Furthermore, the immunoblot shows the lysate fraction only in the asynchronous fraction. Thus, despite Cdt1 still interacting with TIF1γ, the reduced protein lysate levels suggest it may be degraded during mitosis. In contrast, the lysate fraction seen in figure 3.6.2. shows much increased levels of Geminin in the mitotic cells compared with the asynchronous cells.

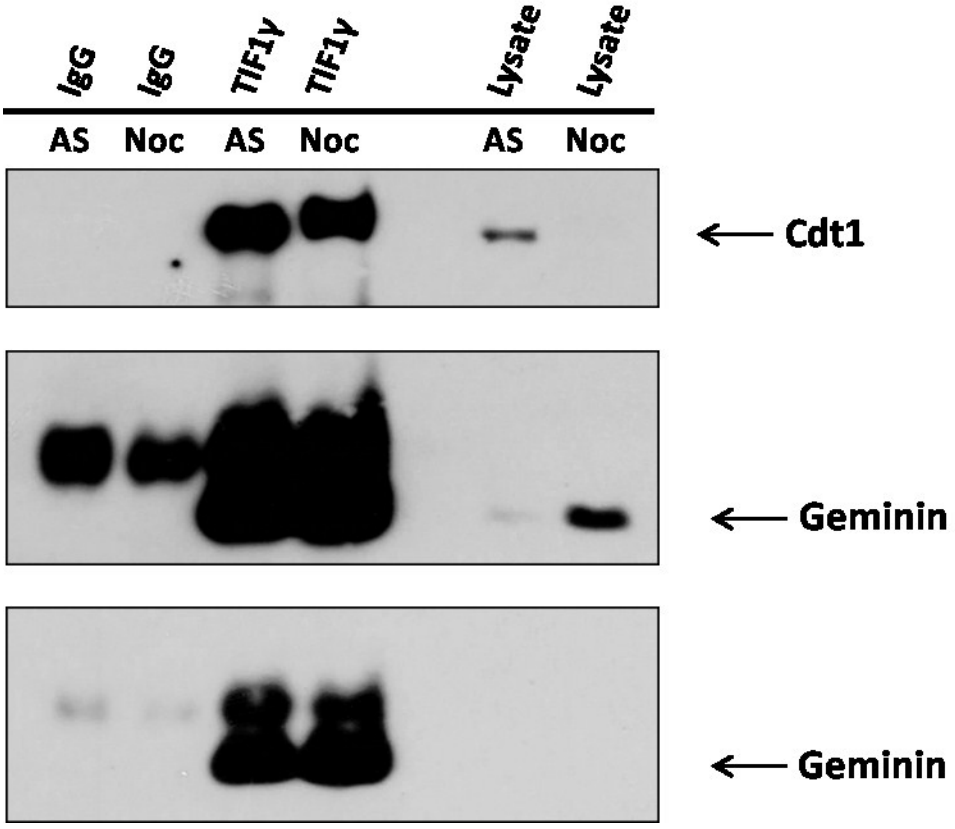

Figure 3.6.2. Immunoblot of TIF1γ-interacting proteins Cdt1 and Geminin from asynchronous and mitotic TIF1γ immunprecipitates -HeLa cells were either left untreated (AS) or subjected to nocodazole treatment (Noc) to induce mitotic arrest and then harvested in NETN lysis buffer. TIF1γ was immunoprecipitated with bound proteins which were then incubated with Protein G-sepharose beads and later eluted. Eluted proteins run on SDS-PAGE were examined by western blotting for the presence of, the TIF1γ-interacting proteins of interest, Geminin and Cdt1.

4. Discussion

In this project we aimed to further investigate TIF1γ interactions within the cell cycle by identifying post translation modifications and novel TIF1γ-interacting partners during mitosis.

4.1. TIF1γ phosphorylation

Firstly in figure 3.1 we identified a shift in TIF1γ mobility on SDS-PAGE during mitosis implying TIF1γ may increase slightly in molecular weight during this stage of the cell cycle. This suggested that TIF1γ may be regulated by post translational modifications during mitosis through processes such as phosphorylation, acetylation or methylation. As phosphorylation is a common process for protein regulation we predicted that this may be the modification seen. By adding λphosphatase to anti-TIF1γ immunoprecipitates we could see that the mobility of TIF1γ was increased compared to in untreated anti-TIF1γ immunoprecipitates (figure3.3). As the shift is reversed when adding a phosphatase it suggests that during mitosis TIF1γ is post translationally modified by phosphorylation. To further support this it may have been useful to repeat this experiment with asynchronous cells as a control.

We also examined whether DNA damage induced by UV or HU treatment stimulated a similar post translational change to TIF1γ. Our results appeared to show no change to TIF1γ mobility over a 6 hour time period suggesting that TIF1γ is not phosphorylated in response to DNA damage. To confirm that the UV and HU treatment did induce DNA damage and subsequently activate DNA damage response pathways we also blotted for pChk1. Previous studies have shown that Chk1 plays an important regulatory role in the G2/M and S phase DNA damage checkpoints. On detection of such damage Chk1 is

phosphorylated by the transducers ATM and ATM-Rad3-related (ATR) and stimulates checkpoint pathways to delay mitotic entry or arrest DNA replication [41]. Our results indicate an increase in pChk1 after UV and HU treatment, implying a DNA damage response was induced despite no obvious changes to TIF1γ mobility. Therefore these changes suggest that TIF1γ phosphorylation may be specific to mitosis.

To further investigate our findings that suggest TIF1γ is phosphorylated during mitosis we expressed asynchronous and mitotic cells with FLAG-tagged TIF1γ derivatives. Interestingly, our results appear to show that when TIF1γ is missing its PHD-Bromo domain it appears to no longer be phosphorylated during mitosis. As phosphorylation appears to occur in the other TIF1γ derivatives these results suggest that the mitotic phosphorylation site resides in the PHD-bromo domain of TIF1γ. However, we found that when expressing cells with just the PHD-Bromo domain mitotic cells did not appear to be phosphorylated. As we proposed that the phosphorylation site was held in this domain these findings were unexpected. These results may be explained by the possibility that key binding sites for TIF1γ-interacting proteins may be held in other domains and therefore the interacting proteins are unable to phosphorylate the TIF1γ PHD-Bromo domain without these other domains present. Given that previous studies have shown the PHD-Bromo domain of TIF1γ is important in binding chromatin, specifically histone H3 tails, it would be interesting to see if phosphorylation of TIF1γ affects its ability to bind chromatin [40]

From MS analysis we identified three TIF1γ phosphorylation sites at amino acids 856, 862 and 1119 of the primary structure. The 862 and 1119 phosphorylation sites were detected in both asynchronous and mitotic cells; therefore phosphorylation of TIF1γ at these sites may be important in alternative regulatory roles outside of mitosis. Conversely the 856 phosphorylation site was only detected in the mitotic cell fraction; as a result this suggests

that this site may be where the phosphorylation modification seen during mitosis in our previous results. Site directed mutagenesis of these phosphorylation sites would have provided confirmation of our suggestions as well as offer further understanding of the roles these specific sites play in TIF1γ mediated cell cycle control. Unfortunately we were unable to isolate colonies for mutagenesis screening and therefore we could not further investigate these findings.

4.2. TIF1γ-interacting proteins

From the MS and IP analysis we showed that Geminin and Cdt1 interact with TIF1γ. This interaction was of particular interest as previous studies have shown that Cdt1 and Geminin interact with each other in order to regulate DNA replication and licensing [41][43]. The proteins play a complementary role in modulating replication; which is an essential process to prevent re-replication of DNA. Cdt1 activity is key in regulating DNA licensing for replication and Geminin acts as a natural inhibitor of Cdt1. To minimise the chances of re-replication Geminin is only degraded for a short period during the cell cycle phases S/G2 and therefore the Cdt1 regulated DNA licensing pathway is only activated briefly. As both Geminin and Cdt1 interact with TIF1γ it is possible that TIF1γ also plays a role in regulating DNA replication [41].

Furthermore, our results showed that Cdt1 may also be post translationally modified in mitotic cells. Previous studies have shown Cdt1 is a substrate of cyclin dependent kinases (cdk); which phosphorylate Cdt1 and subsequently target it for degradation by the SCF-(Scp2) ubiquitination pathway [43]. Therefore the modification to Cdt1 seen in the mitotic cells may be explained by phosphorylation as cdk levels are high in nocodazole arrested cells. Our results further support this reasoning as the lysate fraction of the nocodazole

arrested cells showed much lower expression compared to the asynchronous fraction suggesting that Cdt1 is degraded during mitosis.

4.3. Limitations

Whilst some conclusions have been drawn from the data presented in this study it is important to acknowledge that the short duration of this study means that many of these results would need to be repeated to increase reliability. Moreover, as the MS data was attained at the latter part of the project, time only permitted initial investigation of a couple of proteins we decided were of most interest. Further investigation of the proteins identified by MS would have been ideal to determine whether their interactions with TIF1γ were essential for correct functioning of either protein within the cell cycle.

Unfortunately we were unable to complete the site directed mutagenesis work which would have been useful to determine the function of the TIF1γ phosphorylation sites identified by MS. Although multiple attempts were made using different bacterial strains and PCR conditions we were unable to grow mutated colonies. As we were unable to establish the reason for this we concluded that the experiment would need to be repeated using a new mutagenesis kit.

In addition, although the results compare mitotic arrested cells to asynchronous cells it is key to acknowledge that the asynchronous cells do still have a proportion of cells in mitosis. Therefore, when using highly sensitive techniques such as MS, interacting proteins and phosphorylation sites identified in the asynchronous control fraction may be due to the mitotic cells.

4.4. Future work

Further to the work carried out in this project it would be interesting to investigate the interactions of some of the other proteins identified, in table 3.5, by MS as TIF1γ-interacting proteins. It would also be of interest to continue with the phosphorylation studies now that the potential TIF1γ phosphorylation sites have been identified. Successful completion of the site directed mutagenesis of the identified phosphorylation sites, would allow us to investigate differences in cell cycle functioning between cells expressing WT TIF1γ and mutant forms of TIF1γ. This would also be useful to determine whether the phosphorylation of TIF1γ seen in mitosis is required for successful binding of interacting proteins.

To further establish the functional consequences of TIF1γ phosphorylation, in regards to cell cycle progression and DNA replication, siRNA targeting TIF1γ could be used to knockdown endogenous TIF1γ. This could then be followed by the addition of exogenous plasmids expressing siRNA resistant wild type or mutant TIF1γ to elucidate the cellular effects.

Furthermore, it would be interesting to identify mitotic kinases that phosphorylate TIF1γ in mitosis using *in vitro* kinase assays. Assessing the activity of kinases commonly associated with mitosis such as cyclin b1-cdk1, polo-like kinase 1 (PLK-1), Auroura A and B kinase [44][45][46] after the addition of TIF1γ may provide further understanding of the role TIF1γ plays in mitosis. Moreover, it would also be useful to look at TIF1γ interactions specifically in other cell cycle stages.

TIF1γ has been seen to play numerous roles within the cell cycle. Better understanding of TIF1γ-interactions and regulatory importance may help provide new molecular targets for novel therapies against diseases such as cancer.

5. References

1. Hanahan, D. & Weinberg, R. The hallmarks of cancer. *Cell***100**, 57–70 (2000)
2. Bell, D. Our changing view of the genomic landscape of cancer. *The Journal of pathology* **220**, 231–43 (2010)
3. Lehman, T. *et al.* Oncogenes and tumor-suppressor genes.*Environmental health perspectives* **93**, 133–44 (1991)
4. Land, H., Parada, L. & Weinberg, R. Cellular oncogenes and multistep carcinogenesis. *Science (New York, N.Y.)* **222**, 771–8 (1983)
5. Duesberg, P. Cancer genes: rare recombinants instead of activated oncogenes (a review). *Proceedings of the National Academy of Sciences of the United States of America* **84**, 2117–24 (1987)
6. Hollestelle, A., Elstrodt, F., Nagel, J., Kallemeijn, W. & Schutte, M. Phosphatidylinositol-3-OH kinase or RAS pathway mutations in human breast cancer cell lines.*Molecular cancer research : MCR* **5**, 195–201 (2007)
7. Kyriakis, J. *et al.* Raf-1 activates MAP kinase-kinase. *Nature***358**, 417–21 (1992)
8. Balmain, A., Gray, J. & Ponder, B. The genetics and genomics of cancer. *Nature genetics* **33 Suppl**, 238–44 (2003)
9. Knudson, A. Mutation and cancer: statistical study of retinoblastoma. *Proceedings of the National Academy of Sciences of the United States of America* **68**, 820–3 (1971)
10. Hainaut, P. & Hollstein, M. p53 and human cancer: the first ten thousand mutations. *Advances in cancer research* **77**, 81–137 (2000)
11. Prives, C. & Hall, P. The p53 pathway. *The Journal of pathology***187**, 112–26 (1999)
12. Satyanarayana, A. & Kaldis, P. Mammalian cell-cycle regulation: several Cdks, numerous cyclins and diverse compensatory mechanisms. *Oncogene* **28**, 2925–39 (2009)
13. Mitchison, T. & Salmon, E. Mitosis: a history of division.*Nature cell biology* **3**, E17–21 (2001)
14. Thadani, R., Uhlmann, F. & Heeger, S. Condensin, chromatin crossbarring and chromosome condensation. *Current biology : CB* **22**, R1012–21 (2012)

15. Calbó, J. *et al.* G1 cyclin/cyclin-dependent kinase-coordinated phosphorylation of endogenous pocket proteins differentially regulates their interactions with E2F4 and E2F1 and gene expression. *The Journal of biological chemistry* **277**, 50263–74 (2002)
16. Ito, M. *et al.* Early chk1 phosphorylation is driven by temozolomide-induced, DNA double strand break- and mismatch repair-independent DNA damage. *PloS one* **8**, e62351 (2013)
17. Wei, W. *et al.* Degradation of the SCF component Skp2 in cell-cycle phase G1 by the anaphase-promoting complex. *Nature* **428**, 194–8 (2004)
18. Yang, Q. & Ferrell, J. The Cdk1-APC/C cell cycle oscillator circuit functions as a time-delayed, ultrasensitive switch. *Nature cell biology* **15**, 519–25 (2013)
19. Foster, S. & Morgan, D. The APC/C subunit Mnd2/Apc15 promotes Cdc20 autoubiquitination and spindle assembly checkpoint inactivation.*Molecular cell* **47**, 921–32 (2012)
20. Liu, J. & Nussinov, R. The role of allostery in the ubiquitin-proteasome system. *Critical reviews in biochemistry and molecular biology* **48**, 89–97 (2013)
21. Orlowski, R. & Dees, E. The role of the ubiquitination-proteasome pathway in breast cancer: applying drugs that affect the ubiquitin-proteasome pathway to the therapy of breast cancer. *Breast cancer research : BCR* **5**, 1–7 (2003)
22. Hatakeyama, S. TRIM proteins and cancer. *Nature reviews. Cancer* **11**, 792–804 (2011)
23. Reddy, B., Etkin, L. & Freemont, P. A novel zinc finger coiled-coil domain in a family of nuclear proteins. *Trends in biochemical sciences* **17**, 344–5 (1992)
24. Meroni, G. & Diez-Roux, G. TRIM/RBCC, a novel class of 'single protein RING finger' E3 ubiquitin ligases. *BioEssays : news and reviews in molecular, cellular and developmental biology* **27**, 1147–57 (2005)
25. Sardiello, M., Cairo, S., Fontanella, B., Ballabio, A. & Meroni, G. Genomic analysis of the TRIM family reveals two groups of genes with distinct evolutionary properties. *BMC evolutionary biology* **8**, 225 (2008)
26. Takahashi, M., Inaguma, Y., Hiai, H. & Hirose, F. Developmentally regulated expression of a human 'finger'-containing gene encoded by the 5' half of the ret transforming gene. *Molecular and cellular biology* **8**, 1853–6 (1988).

27. Grignani, F. *et al.* Acute promyelocytic leukemia: from genetics to treatment. *Blood* **83**, 10–25 (1994)
28. Le Douarin, B. *et al.* The N-terminal part of TIF1, a putative mediator of the ligand-dependent activation function (AF-2) of nuclear receptors, is fused to B-raf in the oncogenic protein T18. *The EMBO journal* **14**, 2020–33 (1995)
29. Venturini, L. *et al.* TIF1gamma, a novel member of the transcriptional intermediary factor 1 family.*Oncogene* **18**, 1209–17 (1999)
30. Zhong, S. *et al.* A RA-dependent, tumour-growth suppressive transcription complex is the target of the PML-RARalpha and T18 oncoproteins. *Nature genetics***23**, 287–95 (1999)
31. Khetchoumian, K. *et al.* Loss of Trim24 (Tif1alpha) gene function confers oncogenic activity to retinoic acid receptor alpha. *Nature genetics* **39**, 1500–6 (2007)
32. Cammas, F. *et al.* Mice lacking the transcriptional corepressor TIF1beta are defective in early postimplantation development. *Development (Cambridge, England)* **127**, 2955–63 (2000)
33. Khetchoumian, K. *et al.* TIF1delta, a novel HP1-interacting member of the transcriptional intermediary factor 1 (TIF1) family expressed by elongating spermatids. *The Journal of biological chemistry* **279**, 48329–41 (2004)
34. Klugbauer, S. & Rabes, H. The transcription coactivator HTIF1 and a related protein are fused to the RET receptor tyrosine kinase in childhood papillary thyroid carcinomas. *Oncogene* **18**, 4388–93 (1999)
35. Aucagne, R. *et al.* Transcription intermediary factor 1γ is a tumor suppressor in mouse and human chronic myelomonocytic leukemia. *The Journal of clinical investigation* **121**, 2361–70 (2011)
36. Vincent, D. *et al.* Inactivation of TIF1gamma cooperates with Kras to induce cystic tumors of the pancreas. *PLoS genetics* **5**, e1000575 (2009)
37. Peng, H., Feldman, I. & Rauscher, F. Hetero-oligomerization among the TIF family of RBCC/TRIM domain-containing nuclear cofactors: a potential mechanism for regulating the switch between coactivation and corepression. *Journal of molecular biology* **320**, 629–44 (2002)
38. He, W. *et al.* Hematopoiesis controlled by distinct TIF1gamma and Smad4 branches of the TGFbeta pathway. *Cell* **125**, 929–41 (2006)

39. Sedgwick, G. *et al.* Transcriptional intermediary factor 1γ binds to the anaphase-promoting complex/cyclosome and promotes mitosis. *Oncogene*(2012). doi:10.1038/onc.2012.501
40. Agricola, E., Randall, R., Gaarenstroom, T., Dupont, S. & Hill, C. Recruitment of TIF1γ to chromatin via its PHD finger-bromodomain activates its ubiquitin ligase and transcriptional repressor activities. *Molecular cell* **43**, 85–96 (2011)
41. Tada, S. Cdt1 and geminin: role during cell cycle progression and DNA damage in higher eukaryotes.*Frontiers in bioscience : a journal and virtual library* **12**, 1629–41 (2007)
42. Liu, Q. *et al.* Chk1 is an essential kinase that is regulated by Atr and required for the G(2)/M DNA damage checkpoint. *Genes & development* **14**, 1448–59 (2000)
43. Nishitani, H. *et al.* Two E3 ubiquitin ligases, SCF-Skp2 and DDB1-Cul4, target human Cdt1 for proteolysis. *The EMBO journal* **25**, 1126–36 (2006)
44. Gavet, O. & Pines, J. Progressive activation of CyclinB1-Cdk1 coordinates entry to mitosis. *Developmental cell* **18**, 533–43 (2010)
45. Golsteyn, R. *et al.* Cell cycle analysis and chromosomal localization of human Plk1, a putative homologue of the mitotic kinases Drosophila polo and Saccharomyces cerevisiae Cdc5. *Journal of cell science* **107 (Pt 6)**, 1509–17 (1994)
46. Fu, J., Bian, M., Jiang, Q. & Zhang, C. Roles of Aurora kinases in mitosis and tumorigenesis. *Molecular cancer research : MCR* **5**, 1–10 (2007)